VOL. 5 No. 5 MAY 1940

Philips Technical Review

DEALING WITH TECHNICAL PROBLEMS
RELATING TO THE PRODUCTS, PROCESSES AND INVESTIGATIONS OF
N.V. PHILIPS' GLOEILAMPENFABRIEKEN

EDITED BY THE RESEARCH LABORATORY OF N.V. PHILIPS' GLOEILAMPENFABRIEKEN, EINDHOVEN, HOLLAND

THE DISTRIBUTION OF THE LIGHT REFLECTED BY DIFFERENT CEILING AND WALL MATERIALS

by Joh. JANSEN.

535.242.44 : 628.93

With indirect illumination, especially from coves along the walls, it is not only the total reflectivity of the surface of the ceiling which is important, but also the distribution of the reflected light in all directions. The chief types of reflection may be related to the usual qualitative characterization of the surface as "dull" or "shiny", "rough" or "smooth". In order to replace this qualitative indication by quantitative information, measurements of the above-mentioned distribution have been carried out on a series of materials at different angles of incidence. A number of results of measurements are given and explained.

The reflectivity of a surface is usually indicated by the coefficient of reflection, *i.e.* the portion of the incident light which is reflected. Besides this total reflectivity, however, in many cases the distribution of the reflected light in different directions also plays an important part. This is especially true when the directions of incidence and reflection make large angles with the normal to the surface. It has for example already been explained in this periodical how the quality of a street lighting system is influenced by this factor [1]). Another striking example is encountered in flood lighting for advertising or decorative purposes. If it were desired to illuminate the front of a white marble building in the usual way by placing searchlights near the foot of the building and directing them obliquely upwards on to the building, it would be found that the desired effect was not attained. The marble surface has, however, a satisfactory reflectivity as is shown by the fact that it appears snow white in the daytime. The explanation is obvious. The marble surface reflects the light specularly to a large extent. When the light falls from above, as is the case in the daytime, it is reflected mainly downward, toward the observer. The light which is projected very obliquely from below upon the building is however reflected chiefly skywards. The general conclusion is that smooth surfaces like marble, polished stone and glass are unsuitable for flood lighting, while rough surfaces, on the other hand, like brick, stucco and the like are very well suited for this kind of illumination.

In the case of indoor illumination also, particularly with indirect lighting, the distribution of the light reflected from the materials may be very important. *Fig. 1* shows a diagram of the ordinary

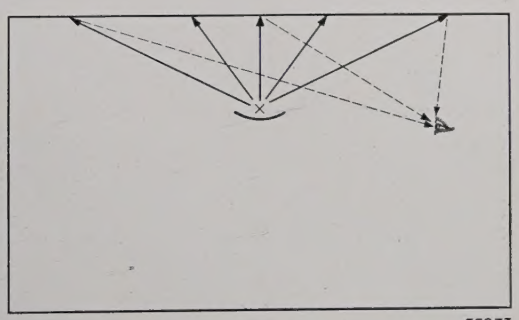

Fig. 1. Indirect illumination with a lamp below the centre of the ceiling.

method of indirect lighting where the source of light hangs below the centre of the ceiling, and radiates its light only toward the ceiling which then as "secondary light source" illuminates the whole room by reflection. It is clear that different parts of the ceiling receive the light at different angles to the normal, some of which are very large, and that an observer sees the different parts from still different directions, some of which diverge very much from the normal. The occurrence of these great variations in angles of incidence and reflection explains

[1]) J. Bergmans, The brightness of road surfaces under artificial illumination, Philips techn. Rev. **3**, 313, 1938.

why the type of reflection of the material of the ceiling in different directions absolutely determines the quality of the illumination. These considerations hold even more strictly when the light sources are

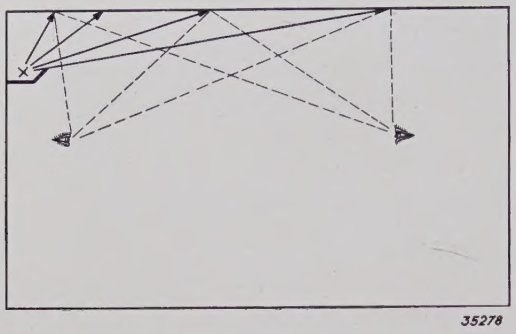

Fig. 2. Indirect illumination with lamps in a cove along the wall. Larger angles of incidence of the light occur here than in the arrangement of fig. 1.

not situated in the centre of the room but along the walls in coves (*fig. 2*). In this case the variations in the angle of incidence are even greater. This type of arrangement is being applied more and more in recent times, since the lack of fixtures hanging from the ceiling promotes a clear view of the room, particularly in long offices [2]) (*fig. 3*).

There has been until now practically no collection of data on the distribution of light reflected by materials of ceiling and walls [3]). Investigations on this subject have been undertaken by the Philips Consulting Bureau on Illumination, and we shall

Fig. 3. Illumination of a long narrow office room by means of coves along a side wall. The absence of lighting fixtures hanging from the ceiling makes possible a clear view of the whole room.

[2]) The fact that in this arrangement the lamps must only radiate light in a relatively small solid angle is no objection thanks to the technical devices such as silver reflectors, "Cornalux" lamps, etc.

[3]) Measurements of this kind have indeed been carried out on various kinds of building stones for outside walls in connection with the above-mentioned question of floodlighting: F. Benford, Gen. El. Rev. **8**, 424, 1928.

here give some of the results. First, however, we shall give a more general discussion of indirect illumination and the influence exerted by the reflective properties of the ceiling.

Qualitative characterization of reflection

The aims of indirect illumination may be outlined as follows:

1) In order to avoid glare it is desirable to remove the light sources with their intense brightness from the field of vision of the user.

2) In order to avoid unpleasant contrasts and shadows it is desired that surfaces other than the working surface should be given an adequate and uniform brightness. The surfaces to be considered are walls and ceiling.

3) An adequate intensity of illumination is desired on the working surface. It is desirable that the power to be installed should not be excessively great.

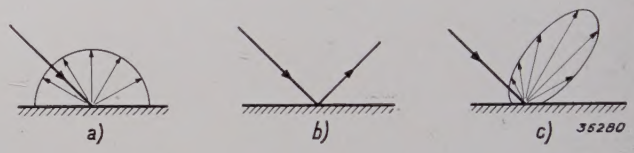

Fig. 4. Distribution of the brightness over all directions with different forms of reflection.

a) Absolutely diffuse reflection according to Lambert's law; the brightness is equally high in all directions.

b) Specular reflection; the brightness is zero in all directions except where the angle of reflection is equal to the angle of incidence. In this direction the brightness is equal to that of the light source.

c) Mixed reflection; the brightness exhibits a more or less pronounced maximum in the direction of specular reflection.

The first requirement is satisfied by the arrangements of figs. 1 and 2 if the sources of light are not below eye level. For point 3) the first requirement is of course a light colour and a high reflectivity of the ceiling. If we now consider a given spot on the ceiling then, according to point 2), it is desired that we should see this spot equally bright from every position in the room. The reflection of the ceiling material should therefore satisfy Lambert's law (entirely diffuse reflection), see the brightness curve *fig. 4a*. For the sake of contrast the distribution of brightness with specular reflection is shown in fig. 4*b*. In practical cases one is usually concerned with intermediate forms of these two extreme cases, a more or less directed reflection (mixed reflection) with for instance a brightness curve like that given in fig. 4*c*.

While in the ideal case of fig. 4*a* a variation in the angle of incidence has no effect on the distribution of brightness, in the case of the more or less directed reflection of fig. 4*c* such an effect must certainly be taken into account. Particularly with large angles of incidence (greater than 45°, for instance) such as occur in a system like that of fig. 2, considerable differences may be expected in this respect, in the sense that with increasing angle of incidence specular reflection will become more and more dominant. This is detrimental not only to the second of the above-mentioned aims, but also to the first and third, because the very bright mirror image of the light source upon the ceiling may be disturbing, and the specularly reflected light can in general only contribute to the effective illumination after several reflections and thus in a considerably attenuated form.

A surface which reflects diffusely we shall call dull, a surface with specular reflection shiny. In addition to this distinction which is based upon the microstructure of the surface, there is also a distinction based upon the macro-structure which is important for reflection phenomena, and which we shall indicate by the terms "rough" and "smooth". A rough surface consists of grains visible to the naked eye which can cast pronounced shadows like miniature hills. On a smooth surface the grains are so small as to be below the limit of visibility. If the light falls perpendicularly on a rough surface, there will be no shadows, with oblique incidence, however, the irregularities cast visible shadows from a given angle (corresponding to the slope of the miniature hills) onwards, and these shadows may give the ceiling a granular appearance (*fig. 5*). The dependence of the reflection on direction in indirect illumination due to the oblique position of the reflecting surfaces will be manifested in a different way than if all the surfaces were horizontal, while a decrease in the total reflectivity may be expected due to the repeated reflection of light between the miniature hills. This last effect becomes even clearer when the rough surface has a fibrous structure, in which case light is captured in the depression of the surface. We shall encounter an example of such a surface later in this article.

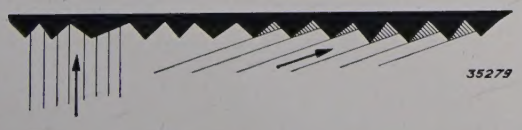

Fig. 5. The effect of shadows of the irregularities of a rough surface.

It is obvious that a smooth surface may be either dull or shiny. But a rough surface may also have both properties. By applying an enamel lacquer to a rough base a shiny rough may easily be obtained. Specular reflection is obtained, but in a different direction for each point. Such a "broken reflection" may in the main correspond to a form of mixed reflection.

Quantitative determination of the distribution of the reflected light

In order to replace this qualitative description of the behaviour of various reflecting surfaces by quantitative data, the measuring apparatus shown in *fig. 6* was constructed. By a lamp L and a lens O_1

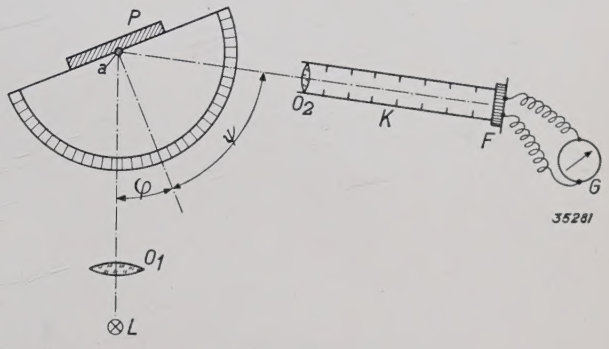

Fig. 6. Apparatus for the measurement of the distribution of the reflected light in different directions. By the light source L and the lens O_1 a circular light spot of uniform intensity is projected upon the test plate P. By turning the plate around the axis a the angle of incidence φ is regulated. The light reflected in a direction Ψ is concentrated by lens O_2 on the photoelement F, whose photocurrent is read from a galvanometer G. The tube K, blackened on the inside, prevents any extraneous or scattered light from reaching the photoelement. The angle Ψ is adjusted by turning the measuring arm.

a light spot of about 6 cm in diameter is projected upon the test plate to be investigated. The intensity of illumination is approximately constant within the circumference of the light spot. The test plate is fastened to a shaft so that it can be rotated. On the same shaft is an arm about 1.50 m long to which is attached a lens O_2 which concentrates the light reflected from the test plate on a photoelectric element (a selenium photocell). The photocurrent generated in the latter is measured directly with a galvanometer and provides a measure of the brightness of the test plate in the direction of observation [4]). In order to obtain comparable results the measured brightnesses are in every case recal-

[4]) The image of the test plate formed by lens O_2 always covered the whole opening of the photoelement, even at the largest angles of observation. The apparent surface, the reflected light flux of which contributes to the excitation of the photocurrent, is therefore constant, *i.e.* the photocurrent is proportional to the brightness of the test plate.

culated for the case where the test plate as a secondary light source radiates a total light flux of 1 lumen per sq.m.

By rotating the test plate and measuring arm the angles of incidence (φ) and of reflection (Ψ) of the light can be regulated. In the measurements the values of the parameter φ of 0°, 30° and 60° were chosen as a rule, while Ψ was varied between +70° and −70° (*fig. 7*). The direction of incidence, the

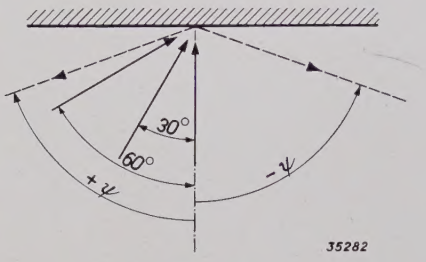

Fig. 7. The angle of incidence φ was set equal to 0°, 30° and 60° successively for all measurements. The angle of reflection Ψ with respect to the normal to the surface investigated is considered positive toward the side of the incident light and was varied between +70° and −70°.

normal to the test plate and the direction of observation always lay in one plane. For the complete calculation of an indirect lighting system the reflection in other planes besides the plane of incidence must of course also be measured. For our present purpose of characterizing different materials, however, the indicated measurements will suffice.

A series of white surfaces which may be used as material for covering ceiling and walls were investigated with the apparatus. As far as possible the same kinds of paint were used on the different surfaces, but were applied by different methods, brushed out smooth or sprayed. The results obtained from six samples are given in *fig. 8a-f*. In addition to the description of the materials used, the total reflectivity (with normal incidence of the light [5])) and the classification according to the qualitative properties given above, two photographs are given of each surface which were taken in such a way that the peculiarities of the surface are presented "in a correct light".

Results of measurements

The samples *a*, *b* and *c* demonstrate the difference between dull and shiny. All three samples were smooth (free of visible irregularities). In the case of sample *a* (dull) the curves which indicate the distribution of brightness are practically circular. This means that, observed in the direction of the light ($\Psi \approx \varphi$) and in the opposite direction ($\Psi \approx -\varphi$), there is little difference. This surface more than all the others investigated most closely approaches the ideal case of reflection according to Lambert's law; the slight deviations at the largest angles are caused by a few local irregularities, accumulations of paint particles, which may be seen as shadow points in the second photograph taken obliquely. The surfaces of samples *b* and especially *c* were not dull but shiny (finished with cellulose lacquer and japan lacquer, respectively). The curves exhibit extremely sharp peaks at $\Psi \approx -\varphi$. The brightnesses in these directions were ten or twenty times higher than in other directions of Ψ. In the photographs also this strongly directed reflection (specular reflection of the light source) may be seen, although because of the limited contrast which can be attained in copying the actual effect is not truly reproduced. For the rest, the brightness in other directions Ψ corresponds approximately to that measured with sample *a*. The light flux at the peaks of the diagrams *b* and *c* is therefore small, and, as far as the efficiency of the illumination is concerned, of little significance [6]). The strong contrasts may however lead to glare.

The other three samples, *d*, *e* and *f* illustrate the effect of a rough surface structure. The test plate *d* was of the same materials as *a* but was tamped, which treatment results in a surface with irregularities about 0.5 mm in height. The diagram shows that the distribution of the reflection over different directions now deviates very much from the circular form. Especially at large values of the angle of incidence φ a considerably greater brightness is observed in the direction of the light ($\Psi \approx \varphi$) than in the opposite direction ($\Psi \approx \varphi$). At $\varphi = 60°$ for instance the two values of the brightness are in the ratio of 2.2 : 1, and at larger angles the ratio increases rapidly. This effect is easily understood from a consideration of fig. 5. With illumination at angles of $\varphi = 45°$, for example, the slopes of the miniature hills which face the source of light are favourable for reflection. Looking in a direction with the light these slopes are clearly seen and the shadow sides are invisible; against

[5]) At other angles of incidence the total reflectivity might have a different value. In the case of the samples investigated, however, the difference for the three parameter values $\varphi = 0°$, 30° and 60° was found to be only very slight (maximum 4%).

[6]) One must not be misled by the fact that the peaks occupy a large part of the area of the diagrams: the area enclosed by these brightness curves has no simple physical significance in particular, this area is not by any means a measure of the total reflected light flux.

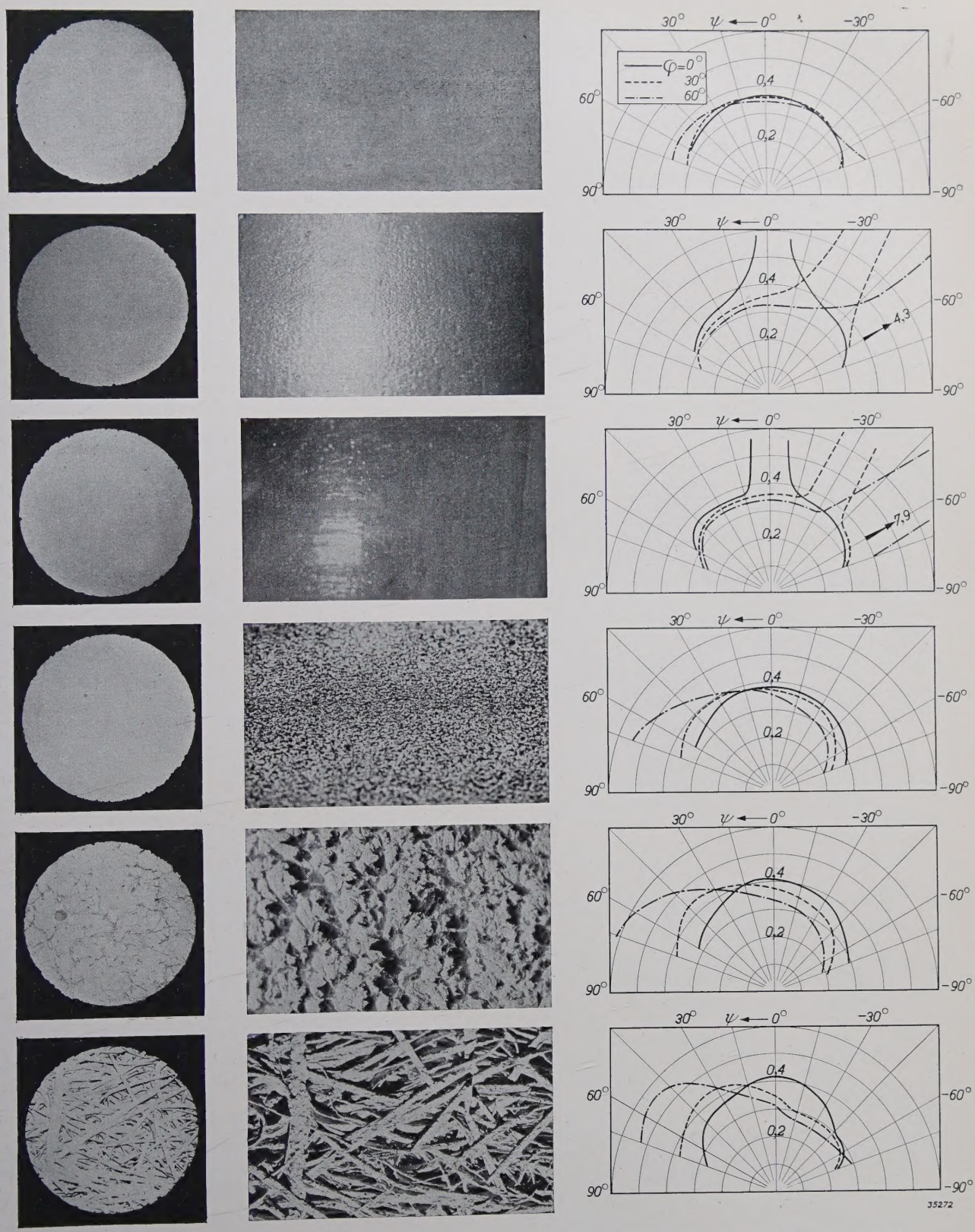

Fig. 8. Photographs and measured brightness distribution of six white surfaces. In the case of the first photograph the angle of incidence φ of the light was always 0°, the angle of observation Ψ = 10-15°. In the second photograph for the samples *a*—*d*, $\varphi = 60°$, $\Psi = 60°$, for samples *e* and *f*, $\varphi = 0°$, $\Psi = 60°$. In the diagrams the brightness is plotted in cp/sq m. which would be observed if a total of 1 lumen of reflected light were radiated per sq.m of the test plate.

a) One coat of priming colour and one coat of size colour; smooth and dull; total reflectivity 86.5% (see note[5])).
b) Two coats of priming colour and one of cellulose lacquer; smooth and fairly shiny; total reflectivity 80%.
c) Two coats of priming colour and one of japan lacquer; smooth and very shiny; total reflectivity 79%.
d) One coat of priming colour and two of size colour tamped; rough (irregularities of 0.5 mm) and dull; total reflectivity 88.5%.
e) Size colour very coarsely tamped; very rough (irregularities of 3 mm) and dull; total reflectivity 82.5%.
f) Size colour on coarse wood fibre board; very rough and dull; total reflectivity 52%.

the light on the other hand one sees only the dark slopes away from the light source and the average brightness observed is therefore much lower.

It must be noted in this connection that wall coverings of the sort *d* (in the form of whitewash or wallpaper) are very common, and that the above-mentioned large angles of observation and incidence are also very important in practical cases (see fig. 2). The consequence is, as the second photograph of sample *d* shows, that the surface appears for a large part covered with shadows. Samples *e* and *f* have a still rougher surface and consequently exhibit the same effect to an even greater degree. In the case of the very irregular fibrous structure of sample *f*, the low reflectivity must moreover be noted (loss of light in the fairly deep crevices of the surface), as well as the irregular shape of the curve representing the distribution of brightness. (This last fact indicates that the cross section of the beam of light which was used for the measurements may here no longer be considered large compared with the irregularities in the structure of the surface being investigated).

Besides the well known fact that with indirect illumination a shiny ceiling must be avoided, the above results show that with a moderately rough structure the ceiling exhibits a maximum brightness in just the opposite direction to that in which the maximum occurs in specular reflection and that with arrangements like the cove systems given in figs. 2 and 3, where angles up to 70 and 80° occur, this effect must be kept clearly in mind. If with such large angles one does not wish to see any disturbing shadows on ceiling and walls, and wishes to attain a satisfactory illuminating efficiency, the surface must be finished as smooth as possible.

This requirement cannot always be satisfied in a simple way. If for example it is required that the ceiling should serve not only as a reflecting plane for the indirect lighting, but that it should also possess sound damping characteristics, we are met with a dilemma; whether to cover the ceiling with a rough or a smooth material. The first is favourable for sound damping and the second is desired for the reflection of light. Which point of view will dominate, or what compromise should be accepted will depend upon circumstances.

When a certain material has been chosen for ceiling and walls, it is possible with the help of brightness curves like those given here, to calculate the effect which may be expected from indirect lighting by means of light sources in certain positions. We hope to be able to discuss this subject at some future time.

ELECTRON TRAJECTORIES IN MULTIGRID VALVES

by J. L. H. JONKER.

537.545.2 : 621.396.694

In the case of tetrodes and pentodes the anode current increases rapidly with increasing anode voltage, and reaches a saturation value at an anode voltage of 20 to 40 volts. It is desirable to make the anode voltage at which saturation occurs as low as possible. For this purpose care must be taken that the electrons are not too much deflected by the wires of the various grids. The deflection of electrons by grid wires and the influence of this deflection on the I_a-V_a characteristic of tetrodes and pentodes is examined theoretically and experimentally in this article. In conclusion the measures are discussed, which can be employed for the purpose of keeping the deflections small.

The properties of transmitting and receiving valves have repeatedly been discussed in this periodical on the basis of diagrams which represent the anode current as a function of the anode voltage, with the control grid voltage as a parameter. In particular the connection has been studied between the maximum output which can be produced under given circumstances and the shape of the I_a-V_a characteristic [1]). Furthermore various installations have been described which were designed for the rapid recording of I_a-V_a characteristics of transmitting and receiving valves. In this article we shall discuss the I_a-V_a characteristics, especially those of multigrid valves, from a more theoretical point of view, and we shall devote special attention to the trajectories of the electrons in the neighbourhood of the grids.

For the sake of orientation the I_a-V_a diagrams of a tetrode and a pentode are again given in *fig. 1*. It may be seen that for a given value of the control grid voltage the anode current at first increases rapidly with increasing anode voltage, and at 20 to 40 volts it has already practically reached its maximum value. In the case of the tetrode the first rapid increase in the anode current is followed by a slight kink due to secondary electrons emitted by the anode which reach the screen grid. In the case of the pentode this kink is absent, since the secondary electrons are driven back by a suppressor grid introduced between screen grid and anode, the wires of which are usually at cathode potential. The secondary electrons in this case therefore return to the anode.

In practical cases where tetrodes and pentodes are used, the object generally is to be able to vary the anode current as widely as possible by a variation of the voltage of the control grid. Since the loading impedance is always included in the anode circuit, changes in the anode voltage naturally also

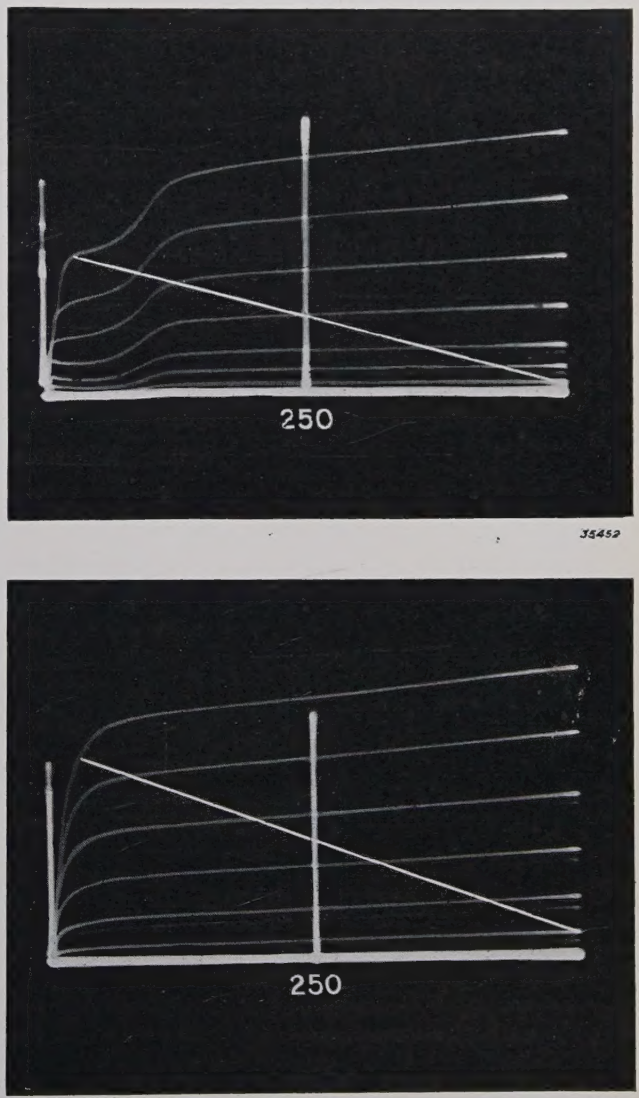

Fig. 1. I_a-V_a characteristics of a tetrode and a pentode. At high anode voltages the anode current is practically independent of the anode voltage. At a certain anode voltage the characteristics of the tetrode exhibit a kink which is caused by secondary emission from the anode.

[1]) For instance in the article: Five electrode transmitting valves, Philips techn. Rev. **2**, 257, 1937.

[2]) In the articles:
Applications of cathode ray tubes, Philips techn. Rev. **3**, 339, 1938;
Recording the characteristics of transmitting valves, Philips techn. Rev. **4**, 56, 1939;
Testing amplifier output valves by means of the cathode, Philips techn. Rev. **5**, 61, 1940.

occur due to this cause, and these changes might affect the variations in the anode current undesirably. As long as the minimum value of the varying anode voltage does not become too low, and the valve continues to operate in the region where the I_a-V_a characteristics is horizontal, the influence of the anode voltage variations on the anode current will only be slight. If, however, the minimum of the anode voltage becomes so low that the neighbourhood of the kink (in the case of the tetrode) or the knee (in the case of the pentode) is approached, the anode current will then increase only very little more, and may even begin to decrease. The curve which represents the anode alternating current as a function of the time for a sinusoidal grid alternating current in this way assumes a very irregular form at the peaks, which may lead to serious distortion.

In order to experience as little difficulty as possible from this disturbance, attempts are made to construct the valves in such a way, that the anode current characteristics remain horizontal to very low anode voltages, and then finally fall at a sharp angle to zero. For this purpose, in systems with cylindrical electrodes, it is necessary in the first place to provide for an accurately centred arrangement [3]), in order that the electrons shall be accelerated and retarded only in radial directions. If this aim were fully achieved the electrons would all attain sufficient kinetic energy, due to the accelerating action of the screen grid, to move counter to the retarding field of suppressor grid and anode at every positive value of the anode voltage, and reach the anode, so that the anode current would reach its maximum value at any given low anode voltage.

Actually, however, the characteristics by no means ever reach this ideal, even with the most careful assembly. The anode voltage at which the anode current reaches its maximum value is always found to amount to 10 per cent or more of the screen grid voltage. It may be concluded from this that, in addition to asymmetry of the assembly, there must be other factors, which have a depressing action on the radial component of the velocity of the electrons.

It has been found that this decrease in radial velocity may be ascribed chiefly to the deflection of the electrons by the wires of the grid.

Due to this deflection the motion of the electrons, which would otherwise be truly radial, is given a tangential component. Since the total velocity does not change (at every point it is given by the value of the potential), the radial component of the velocity of the deflected electrons is smaller than that of the non-deflected electrons. At low anode voltages the electrons which are most strongly deflected, and which therefore move the slowest in radial directions, will be unable to reach the anode against the retarding field of suppressor grid and anode, and it is to this fact that the decrease in anode current with decreasing anode voltage must be mainly ascribed.

In order to test this hypothesis quantitatively, and in addition to investigate to what degree the I_a-V_a characteristics of a pentode can be influenced by structural means, the deflection phenomena of electrons in pentodes have been investigated theoretically and experimentally. By „experimental" investigation we mean here not only measurements carried out on test valves made especially for this purpose, but also a study of the motion of the electrons with the help of models in which the variation of potential in a system is imitated by means of a rubber membrane stretched in a certain way, and the electrons are represented by steel balls rolling across the rubber membrane [4]). We shall begin with a description of the deflection by a positive grid (screen grid), which has also been analyzed theoretically, and will then consider the deflection of the electrons by the control grid and the suppressor grid.

Deflection of electrons by a positive grid

When an electron leaves the cathode with zero velocity it will at first be accelerated by a positive grid in a radial direction, or, when the electrodes are plane, in a direction perpendicular to the cathode. We shall call this direction "radial" in the future for the sake of simplicity. In the neighbourhood of the grid wires, however, the field is no longer truly radial but also contains a tangential component which gives the electron a lateral deflection. The magnitude of this deflection varies according to whether the electron passes midway between two grid wires or closer to one of them. This is illustrated clearly in *fig. 2*, where the electron trajectories are recorded with the help of a rubber membrane for the case of a positive grid, behind which is situated the anode, which is also positive but at a considerably lower potential. The manner in which the deflection which the electrons undergo upon passing the grid varies between two grid wires is clearly shown. It is also clear that the most strongly deflected elec-

[3]) An example of this is given in the last article referred to in footnote [2]).

[4]) This method is described in detail in Philips techn. Rev. **2**, 338, 1937.

trons are unable to reach the anode, so that the anode current is smaller than the electron current which passes through the slits of the screen grid.

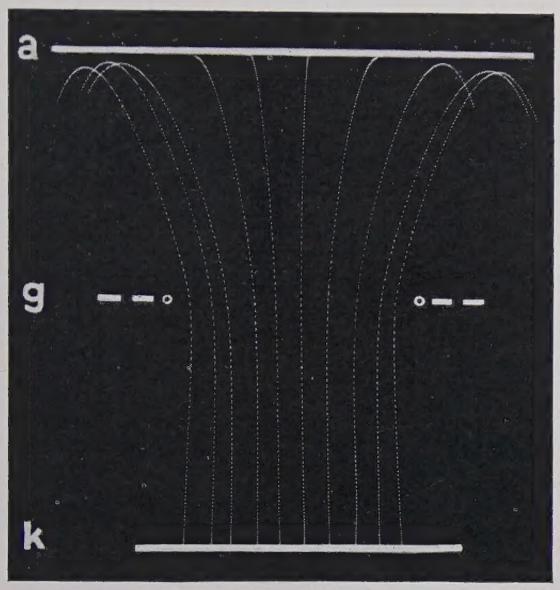

Fig. 2. Electron trajectories between two rods of a plane positive grid followed by an anode plate which is slightly negative. The pictures were obtained by intermittent illumination (50 c/sec) and photographing of balls rolling over a stretched rubber membrane. It may be seen that the strongly deflected electrons do not move as far counter to the anode potential as do the less deflected electrons.

If the anode voltage were gradually increased, the non-deflected electrons would reach the anode first (namely as soon as $V_a > 0$) and only at a considerably higher voltage would all the electrons reach the anode.

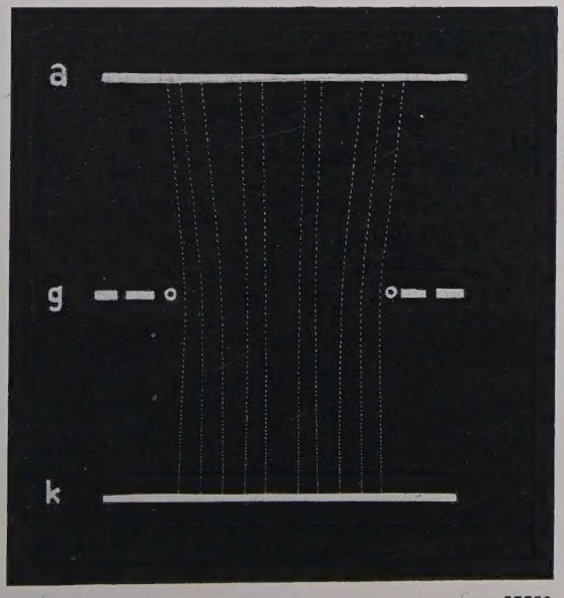

Fig. 3. Electron trajectories between two rods of a plane positive grid followed by an anode at the same potential. This figure is more suitable than fig. 2 for determining the angles of deflection.

In order to be able to measure the angles of deflection of the different trajectories easily it is desirable to choose the circumstances so that the trajectories are straight lines behind the positive grid. This can be achieved simply by giving the anode the same potential as the grid. *Fig. 3* shows the electron trajectories obtained in this way, while in *fig. 4* the results are given which may be deduced from that figure, namely the angle of deflection as a function of the point at which the electron passes the positive grid.

It is immediately obvious that the tangent of the angle of deflection is almost directly proportional to the coordinate x, which indicates at what distance from the middle of the slit between two grid wires the electron traverses the plane of the grid.

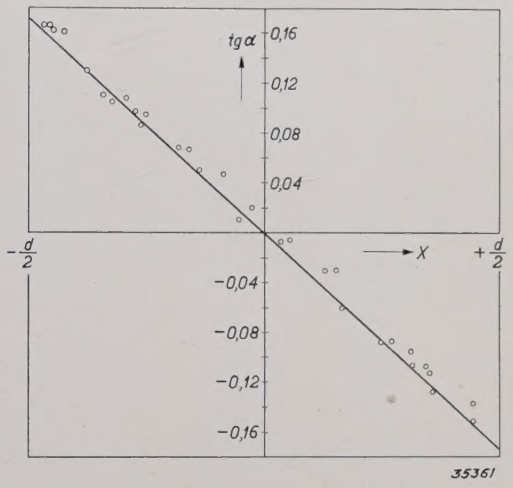

Fig. 4. Tangent of the angle of deflection as a function of the point relative to two grid wires where the electron traverses the grid. Midway between two wires ($x = 0$) no deflection occurs, to the left and right of the middle point the electrons are deflected in opposite directions through an angle whose tangent is proportional to the distance from the middle.

If the maximum angle of deflection α_m for electrons which pass the grid wires as close as possible ($x = d/2$) is known, then by using this relation, the anode current I_a can immediately be calculated which will occur at a given value of V_a when a homogeneous beam of electrons corresponding to a current I_a passes between the grid wires. As may be seen from fig. 2 all the electrons cannot reach the anode at a low anode voltage, but only those whose angle of deflection does not exceed a certain value which we shall call α_0. A certain value of the coordinate x_0 corresponds to this angle α_0, and consequently a certain current, which is given by the following [5]):

[5]) Since the theoretical considerations hold only for small angles, we may in qualitative discussions neglect the difference between the angle itself and its functions sin α and tan α.

$$\frac{I_a}{I_k} = \frac{x_0}{d/2} = \frac{\tan \alpha_0}{\tan \alpha_m} \sim \frac{\alpha_0}{\alpha_m} \quad \cdots \quad (1)$$

α_0 depends upon the grid voltage V_g and the anode voltage V_a. If the anode voltage is equal to zero (cathode potential), then only those electrons can reach the anode which are entirely undeflected. α_0 thus becomes equal to zero, and the same holds for the anode current. With increasing anode voltage α_0 becomes steadily larger, and finally reaches the value α_m, which means that all the electrons which pass through the slits of the screen grid also reach the anode.

What is the relation between α_0, V_a and V_g? The electrons which pass through the slits of the screen grid (potential V_g) have a velocity v which is determined by $^1/_2\, mv^2 = eV_g$ where m is the mass and e the charge of an electron. From this it follows that:

$$v = \sqrt{2\,\frac{e}{m} V_g}.$$

For electrons which are deflected through an angle α_0 the radial velocity v_r is smaller than v and equal to $v \cos \alpha_0$. Their kinetic energy in a radial direction is therefore

$$^1/_2\, mv_r^2 = {}^1/_2\, m\, \frac{2e}{m}\, V_g \cos^2 \alpha_0 = e\, V_g \cos^2 \alpha_0.$$

These electrons which are deflected through an angle α_0 will just be able to reach the anode when their kinetic energy in a radial direction corresponds to the potential difference between grid and anode, thus when:

$$e\, V_g \cos^2 \alpha_0 = e(V_g - V_a), \text{ or}$$
$$V_a = V_g\,(1 - \cos^2 \alpha_0) = V_g \sin^2 \alpha_0.$$

For small angles of deflection we find from this

$$\alpha_0 \sim \sin \alpha_0 = \sqrt{\frac{V_a}{V_g}},$$

and by substituting this value of α_0 in equation (1) for the anode current we find:

$$\frac{I_a}{I_k} = \frac{1}{\alpha_m} \sqrt{\frac{V_a}{V_g}} \quad \cdots \quad (2)$$

The result is therefore that the anode current I_a at a given screen grid voltage V_g is proportional to the square root of the anode voltage V_a. This is of course only valid for low anode voltages, for which $\alpha < \alpha_m$. When $\alpha_0 = \alpha_m$, in other words when

$$V_a = V_g\, \alpha_m^2,$$

all electrons reach the anode; the I_a-V_a characteristic has a kink, and then continues horizontally with increasing anode voltage.

Before applying the theoretical conclusions to the usual types of construction for practical use, we shall first consider the value of the maximum angle of deflection α_m.

Calculations have been carried out by Below [6]) on the maximum angle of deflection α_m. He considered the electron trajectories in the neighbourhood of a plane grid for the case when the grid potential is high compared with the fluctuations in potential within the region around the grid where the deflection occurs, so that it is permissible to assume that all the electrons pass the plane of grid with the same velocity.

As a result of his calculations follows in the first place the linear relation between the position where the electron passes the grid and the deflection, as was found experimentally in fig. 4. For the maximum angle of deflection he also obtained the following relation:

$$\tan \alpha_m = \frac{\pi \gamma}{V_g}, \quad \cdots \quad (3)$$

where γ is the charge per cm of grid wire.

The charge is determined by the capacity and the potential difference between the grid and the adjacent electrodes, which we have called cathode and anode for the sake of simplicity. The capacities can be calculated approximately by considering the grids as cylindrical or plane electrodes with a certain effective potential. The charge found in this way must then be recalculated per cm of the grid wire. For this purpose the total length l of the grid wire is calculated from the pitch and the radius of the grid, and the charge is then divided by l. The result of these calculations, which we shall not describe in detail, is the following for the case of cylindrical electrodes:

$$\tan \alpha_m = \frac{d}{4 r_g V_g} \left(\frac{V_g - V_k}{\ln \frac{r_g}{r_k}} + \frac{V_g - V_a}{\ln \frac{r_a}{r_g}} \right), \quad (4)$$

where d is the distance between successive wires of the control grid, and r_k, r_g and r_a are the radii of cathode, grid and anode, respectively. For the case of plane electrodes the formula becomes:

$$\tan \alpha_m = \frac{d}{4\, V_g} \left(\frac{V_g - V_k}{a_{gk}} + \frac{V_g - V_a}{a_{ga}} \right), \quad (5)$$

where a_{gk} and a_{ga} represent the distances between

[6]) F. Below, Z. Fernmeldetechn. **9**, 113-136, 1928.

the grid and the cathode and the grid and the anode respectively. Together with equation (2) equations (4) and (5) give the anode current as a function of the anode voltage and the grid voltage.

Equation (5) can be tested experimentally by measuring the maximum deflection for a number of different electrode configurations by means of a rubber membrane, and comparing the result with the calculation. This check gives quite satisfactory results. The measured deflections are found to agree within 8 per cent with the calculated deflections, as follows from *table I* where a number of cases are summed up. Since there are certain errors in the method of measurement with a rubber membrane [7]), and also since Below's theory is exact only for small angles of deflection, a better agreement could not be expected.

Table I. Deflection of electrons by a positive grid between two electrodes at zero potential.

	Dimensions of the model (cm)				tan α_m	
	a_{ga}	a_{gk}	d	diametre of grid bars	measured	calculated
I	10	10	10	1,0	0,180	0,179
II	20	20	20	1,9	0,188 0,182*	0,177
III	20	20	20	1,0	0,150 0,170	0,158
IV	10	30	10	1,0	0,188 0,183	0,199
V	10	30	5	1,0	0,107 0,123	0,114

* Two measurements being made for the models II—V.

Having shown in this way that the deflection of electrons by the screen grid can be calculated with sufficient accuracy, it would seem obvious that the I_a-V_a characteristics of existing valves can be calculated with the help of the formulae found, and that means of making the shape of these characteristics as satisfactory as possible can be considered. This would indeed be possible if the screen grid were the only electrode which causes a deflection of electrons. In the case of electronic valves of practical importance, however, in addition to the screen grid there is always a control grid and often a suppressor grid also, and these grids may also cause a deflection of the electrons which is found in practice not to be small compared with the deflections caused by the screen grid.

These additional deflections of the electrons by suppressor and control grid cause the anode current to reach its maximum value with increasing anode voltage later than would follow from the theory discussed in the foregoing. Moreover, due to these extra deflections, the shape of the I_a-V_a curve is very much altered in the neighbourhood of the knee. In order to deal with this in detail we shall first investigate the deflection of electrons at the control grid and suppressor grid, respectively, particularly for the simple case where the wires of these grids are at cathode potential.

In the case of the suppressor grid this is practically always the case. The wires of the control grid, on the other hand, usually have a negative potential; zero potential only occurs as a maximum value. Since we are in the first place interested in the shape of the I_a-V_a characteristic at low anode voltages, it is just this maximum control grid voltage with which we are concerned; on the load line the lowest anode voltage corresponds to the highest control grid voltage (see fig. 1).

Deflection of electrons by a grid at zero potential

In the case of a grid at zero potential situated in the neighbourhood of another electrode at a high potential (the screen grid) the condition is no longer fulfilled that the fluctuations in potential in the plane of the grid shall be small compared with the average potential which determines the velocity of the electrons. The velocity of the electrons which reach the slit between two grid wires can no longer be considered independent of the position, but is now considerably greater at the middle of the slit than in the neighbourhood of the grid wire. This is shown clearly in the shape of the electron trajectories as found with the help of the stretched rubber membrane (see *fig. 5*). If the conditions of the above discussed theory were satisfied, then at every point on the grid the tangent of the angle of deflection would be proportional to the distance between that point and the middle of the slit. But in that case the deflection would be opposite in direction to that with a grid at a high potential,so that the electrons would be focussed to a point. Since, however, contrary to the theoretical assumption, the electrons move slower and slower with increasing distance from the middle, so that the deflection is greater than demanded by the theory, the focal distance for electrons on the

[7]) See the article referred to in footnote [4]).

edges of the slit is shorter than for those at the middle of the slit. In optical language, the slit between two grid wires forms a cylindrical lens with a positive spherical aberration.

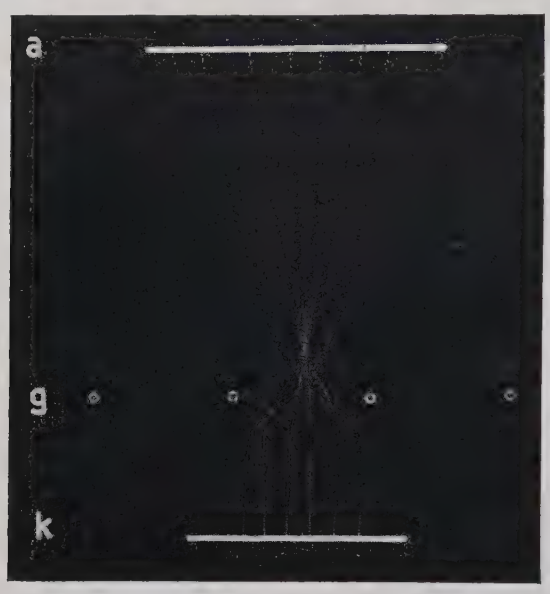

Fig. 5. Trajectories of electrons at the moment of passing a grid at zero potential. The deflection is in the opposite direction to that in fig. 2: the beam of electrons is not spread, but focussed.

Since the angle of deflection of the sharply curved electron trajectories in the neighbourhood of the control grid is difficult to determine from the figure, the angle of deflection α of the electron at the anode is measured instead, and this deflection differs only by a constant factor from the control grid deflection. For the same reason the coordinate x was not determined in the plane of the grid but in the plane of the cathode.

If $\tan \alpha$ is once more plotted as a function of x, then on the basis of the experiments with the rubber membrane the curve given in *fig. 6a* is obtained. Over one half the width of the slit on either side of the middle the curve is practically a straight line, but closer to the grid wires the deflection increases more rapidly than proportional to the distance from the centre line. Close to the grid wire the deflection begins again to decrease because the first deflection is so great that the electrons come under the influence of the adjacent grid wire and are deflected in the opposite direction.

The straight line *b* in fig. 6 represents the deflection which is calculated theoretically on the assumption (actually an incorrect one) that the variations of the potential in the plane of the grid are small compared with the effective grid potential. By combining equations (2) and (5) the following formula is obtained for the angle of deflection α:

$$\tan \alpha = \frac{2x}{d} \frac{d}{4V_{g1}} \left(\frac{V_{g1}-V_k}{a_{g1k}} + \frac{V_{g1}-V_{g2}}{a_{g1g2}} \right), \quad (6)$$

The agreement of the lines calculated with (6) and the curve deduced from the measurements is rather better than might be expected taking into account the rough considerations used; the decrease in the experimental deviation for great values of x has an important influence on this result.

As this formula can be applied with space discharge grids, as well as with secundary emission grids, the deviation phenomena for any grid in tetrodes or pentodes can be described with formula of similar shape.

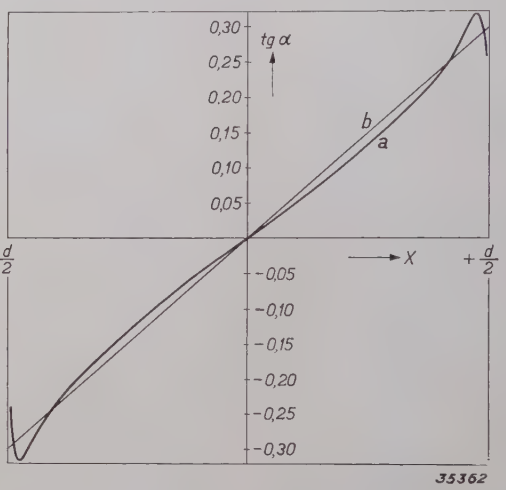

Fig. 6. Tangent of the angle of deflection of electrons which pass a grid at zero potential as a function of the distance between the starting point of the electron and the line half way between two grid wires, α is the angle at which the deflected electrons reach the anode.
a) Experimentally determined curve;
b) Curve calculated on the assumption of a constant potential in the grid plane equal to the average grid voltage.

I_a-V_a characteristics of tetrodes and pentodes

After having accounted for the deviating properties of the individual grids of a tetrode or a pentode, we now can indicate the partition of electrons for different angles of deviation, if these electrons have passed all the grids of a tetrode or a pentode. From this angular partition the I_a-V_a characteristic of the tube can be calculated in a similar manner as used in the given considerations for the angular partition of electrons reflected at the screening grid. With very small anode voltages, in which we are interested here, this picture will agree with the facts, however, this is not the case with greater anode voltages *i.a.* because we neglected the electrons which after having passed the screening grids, are partially lost for the anode current, by

direct reflection on the wires of the space discharge grid.

The cooperation of these deviations in the different grids may occur in various manners. If *e.g.* two successive grids have the same pitch, the electrons which are deviated by the first grid cannot be distributed uniformily over the openings of the next grid, it therefore matters, if the wires of the second grid are placed in line with the wires of the first grid, or if they have a displacement of half the pitch with respect to those of the first one. In the following the first case shall be considered more in detail.

For the present, however, we assume that the grids are unequal in pitch, and therefore that the lateral components of the velocity which are due to the deflection at the three grids may be added together according to the laws of chance.

The tangential component of velocity which is imparted to the electron in the plane of each grid is equal to the total velocity in the plane of the grid multiplied by the sine of the angle of deflection. In this manner one finds with the aid of form. (5) and (6) for the tangential changes in velocity, which the electrons undergo in each of the three grids of a pentode the following:

$$\left.\begin{aligned} v_1 &= \sqrt{\frac{e}{2m}}\, x_1 \frac{1}{\sqrt{V_{g1}}}\left(\frac{V_{g1}-V_k}{a_{g1k}} + \frac{V_{g1}-V_{g2}}{a_{g1g2}}\right), \\ v_2 &= \sqrt{\frac{e}{2m}}\, x_2 \frac{1}{\sqrt{V_{g2}}}\left(\frac{V_{g2}-V_{g1}}{a_{g1g2}} + \frac{V_{g2}-V_{g3}}{a_{g2g3}}\right), \\ v_3 &= \sqrt{\frac{e}{2m}}\, x_3 \frac{1}{\sqrt{V_{g3}}}\left(\frac{V_{g3}-V_{g2}}{a_{g2g3}} + \frac{V_{g3}-V_a}{a_{g3a}}\right). \end{aligned}\right\} \quad (7)$$

x_1, x_2 and x_3 are here the chance position coordinates in each grid, and they may vary from zero to half the pitch. V_{g1}, V_{g2} and V_{g3} are the average potentials in the three grid planes, as in the foregoing. The total tangential component of the velocity behind the suppressor grid is $v_1 + v_2 + v_3$.

If the three expressions in equation (7) are compared it is seen that with normal dimensions of an output pentode they may have about the same order of magnitude. It is therefore quite incorrect to consider only the scattering by the screen grid, for instance, as is sometimes done.

The way in which the three tangential components must be added together is shown in *fig. 7*. It is thereby assumed that $v_1 > v_2 > v_3$. Such an assumption does not detract from the general validity of the analysis, since the total deflection in the approximation in question is independent of the order in which the grids are traversed.

If only the first grid is traversed, all the tangential velocities between $-v_{1\max}$ and $+v_{1\max}$ are present to the same extent in the scattered beam, as indicated in fig. 7*a* (the subscript *max* is omitted in the figure). The diagram has the simple form of a rectangle.

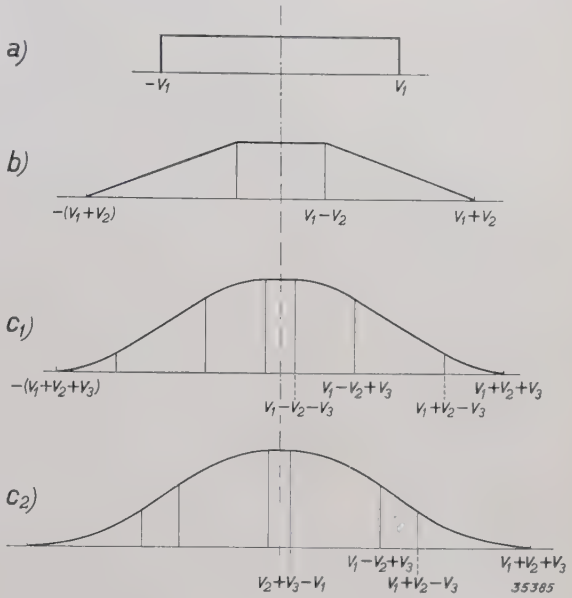

Fig. 7. Distribution of the tangential velocities in a beam of electrons which is scattered by one, two or three grids.

If the beam is scattered by a single grid all tangential velocities between two maximum values $+v_1$ and $-v_1$ occur to the same extent; the distribution of velocities is given by a rectangular diagram (curve *a*).

If the scattered beam is then again scattered by a second grid, the number of electrons per unit of velocity interval is given for every velocity v by the area of curve *a*) between $v-v_2$ and $v+v_2$, where v_2 indicates the maximum tangential velocity imparted to the electron by the deflection at the second grid, which is assumed to be smaller than v_1. In this way the trapezium-shaped curve *b*) is obtained.

If the beam is then scattered once more by a third grid, curve *c*) is obtained, in which the ordinate for every velocity v is given by the area of curve *b*) between $v-v_3$ and $v+v_3$. As to the shape of the curve, a distinction must be made between $v_3 < v_1 - v_2$ (curve c_1) and $v_3 > v_1 - v_2$ (curve c_2). Both curves are composed of parabolic and straight sections. The difference lies in the fact that the middle portion of curve c_1 is horizontal, while in the case of c_2 it is part of a parabola whose curvature is twice as great as that of the other parabolic sections.

If in addition to the first grid the second grid is also traversed, a diagram like that of fig. 7*b* is obtained. All the electrons which have tangential velocities between $v-v_{2\max}$ and $v+v_{2\max}$ after deflection by the first grid now contribute equally to every total tangential velocity v. The number of these electrons can be found by considering the area of the first diagram between $v-v_2$ and $v+v_2$. A trapezium-shaped diagram is obtained as explained in the text under the figure.

If in the same way the scattering by the third

grid is also considered the kinks in the trapezium figure disappear; the diagram becomes a smooth curve composed of straight sections and parabolic curves. As may be seen in fig. 7*c* two cases must be distinguished: namely $v_1—v_2—v_3 > 0$ and $v_1—v_2—v_3 < 0$. In the first case the upper part of the diagram contains a straight section, while in the second case it is parabolic. The shape of the whole curve already shows a certain similarity with the Gauss curve for the distribution of chance fluctuations, and with an increasing number of grids it would soon approach Gauss curve.

After having determined in this way the distribution curve of the tangential velocities for one, two and three grids, we can calculate the I_a-V_a characteristic for each of these cases. It must be kept in mind that at every anode voltage V_a those electrons reach the anode whose tangential velocity after traversing all the grids is smaller than a certain maximum value v_0, which is given by:

$$^1/_2\, m\, v_0^2 = e\, V_a.$$

In *figs. 8a, b* and *c* the characteristics are reproduced which are calculated in this way for the cases of 1, 2 and 3 grids. The case of one grid, as already stated, has no great practical importance; the case of two grids may, at a very low voltage, at which no appreciable secondary emission occurs, be compared with the characteristic of the tetrode, while the diagram for three grids — also only at very low voltages — corresponds to the case of the pentode.

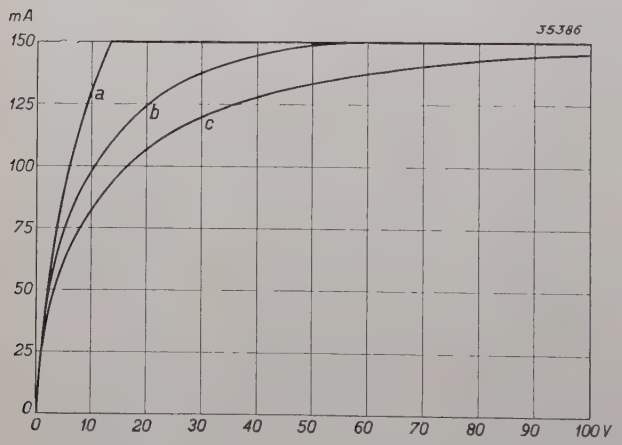

Fig. 8. I_a-V_a characteristics calculated for electron beams which are scattered according to the velocity diagrams of figs. 7*a*, *b* and c_2.

Conclusions as to the construction of tetrodes and pentodes

In order that the anode current may reach its saturation value at the lowest possible anode voltage, it is desirable to make the deflections experienced by the electrons at the grid wires as small as possible. Several conclusions as to the construction of the various grids may be drawn from this requirement.

The control grid

Just as in the case of every grid so with the control grid is the maximum deflection which may occur according to equation (7) proportional to the pitch. It is therefore advisable to make the pitch of the grid small. Since this is done for other reasons also in valves with a steep slope, it is understandable that such valves also have a favourable I_a-V_a characteristic, which fact is manifested in a high value of the ratio between the maximum useful output and the anode dissipation.

If the control grid voltage is strongly negative the electrons cannot pass the grid at any arbitrary spot, but only in a narrow region in the middle of the slits, where the potential in the grid plane is still positive. It is obvious that the deflection of the electrons is hereby weakened, since the deflecting forces are weakest in the middle of the slits. In confirmation of this it is often observed that the knee becomes sharper and sharper with increasing negative control grid voltage.

The screen grid

In the case of the screen grid it would seem better not to make the pitch too low since then the current consumption would become too great. The question arises, however, as mentioned above, whether a decrease in the deflections cannot also be obtained by placing the wires of the screen grid in line with the wires of the control grid.

With satisfactory mutual relations between the pitch and the distance between control grid and screen grid this may indeed bring about an improvement. The electrons are focussed by the control grid, and when the focus does not lie at too great a distance from the screen grid the electrons will tend to pass through the middle of the slits of the screen grid where the deflection is weak. At the same time the screen grid current is hereby diminished and consequently the noise [8]).

Fig. 9 shows the electron trajectories, recorded on a model, through a negative and a positive grid whose wires are placed directly behind one another. As may be seen the deflections which the electrons experience in the two grid planes are not

[8]) This is further explained in: Noise in amplifiers contributed by the valves, Philips techn. Rev. **2**, 329, 1937.

independent of each other: those electrons which are most strongly deflected at the control grid also experience the greatest deflection at the

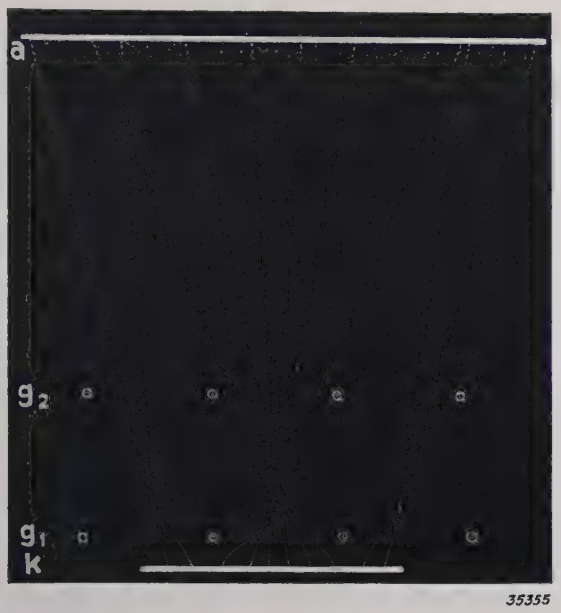

Fig. 9. Electron trajectories for a negative and a positive grid whose wires are situated directly behind each other. The deflection of an electron by the second grid is proportional to the deflection which it has already undergone at the first grid.

screen grid. The deflecting effect of the screen grid in this case may be described by saying that every deflection which the electron undergoes at the control grid must be multiplied by a certain factor. The distribution of the tangential velocities thus remains essentially that of a single grid, so that the I_a-V_a characteristic in this case will have the shape of fig. 8*a* and exhibit a sharp kink. Such a characteristic is indeed found in the case of tetrodes when the wires of control and screen grid are placed directly behind each other.

The suppressor grid

The deflection by the suppressor grid is determined by the third member of equation (7), namely:

$$v_3 = \sqrt{\frac{e}{2m}}\, x_3 \sqrt{\frac{1}{V_{g3}}} \left(\frac{V_{g3} - V_{g2}}{a_{g2g3}} + \frac{V_{g3} - V_a}{a_{g3a}} \right) . \quad (8)$$

As may be seen this expression is composed of two terms which have opposite signs at low anode voltage ($V_a < V_{g3}$). The first term is negative, the second positive. It is obvious that the position and potential of the suppressor grid can be so chosen that the two terms cancel each other. Since in the case in question both V_{g3} and V_a have fairly low values, while the screen grid voltage V_{g2} is high, the numerator of the negative term will be considerably larger than that of the positive term. In order to make the two terms equal in absolute value, the same relation must hold for the denominators, and this means, that the distance a_{ga} between the suppressor grid and the anode must be chosen considerably smaller than that between suppressor and screen grid.

Just as in the case of the control grid and the screen grid, one might in the case of the suppressor grid also attempt to diminish the deflections by making the pitch of the grid low. This device, however, does not produce the desired result. As we

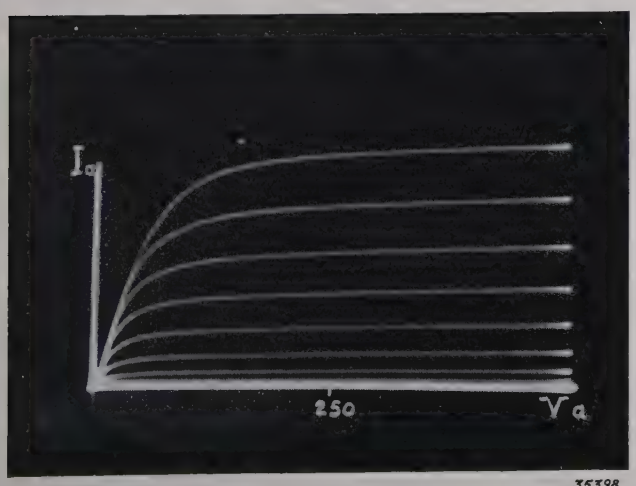

a

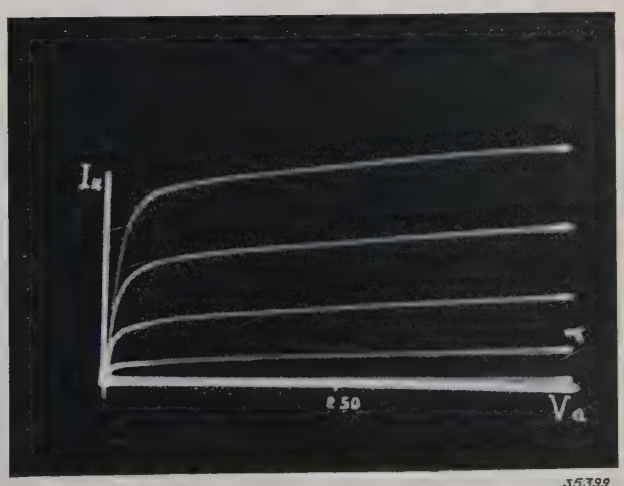

b

Fig. 10. I_a-V_a characteristics of two output pentodes.
a) Earlier type with low slope.
b) Modern type with steep slope, in which the deflections of the electrons have been kept as small as possible by various means. The practically horizontal rectilinear part of the characteristic begins at a much lower anode voltage.

have seen, for a compensation of the two deflection terms it is necessary that the effective suppressor grid potential V_g should lie between those of the screen grid and the anode, because only in that case do the two terms of equation (8) have opposite signs. Since the grid wires themselves are at cathode potential, which is lower than the desired value of the effective potential, it is necessary that the effect of the anode and screen grid should be sufficiently felt between the wires of the grid. Therefore it is of advantage to make the pitch large and to try to keep the deflection small by a suitable choice of the position of the suppressor grid as in the case above.

In *fig. 10* the I_a-V_a characteristics of an earlier and a modern type of pentode (amplifier output valve) are reproduced, from which it may be seen that the flat part of the characteristic could be extended to considerably lower anode voltages. The improvement is obtained mainly be decreasing the pitch of the control grid and by suitable placing of the suppressor grid. The position of the knee in the diagram has been shifted from about 40 volts to about 20 volts.

MICROPHONES

by J. de BOER.

621.395.61

An explanation is given of the different ways in which sound vibrations may be converted in a microphone into vibrations of a membrane, ribbon or plate, which possesses one degree of freedom, and how these vibrations can in turn excite an alternating EMF in an electrical circuit. The considerations provide a basis for the division of microphones into different types. In conclusion several types of microphones are described.

The name microphone was originally used by C. Wheatstone to denote an instrument which served to make very weak sounds audible to the human ear, and which was therefore what we now call a stethoscope. Now, however, the name microphone is used exclusively for instruments which convert air vibrations into electrical AC voltages. The early development of microphones took place during the years 1876 and 1877. At that time Alexander Graham Bell (1876) was laying the foundations of modern telephony. In his work he used a microphone which worked on the electromagnetic principle. One year later (1877) both Thomas Edison and Berliner were granted patents for a much more sensitive microphone, whose action depended upon the variable resistance of powdered carbon. Since that time the further development of the microphone has gone hand in hand with the development of reproduction and recording of sound.

The various kinds of microphones have one feature in common, namely they all first convert the motion of the air particles into motion of a membrane, ribbon or plate. This motion leads to the excitation of an electrical AC voltage, so that the following sequence is always involved:

motion of air → motion of membrane → EMF.

In a sound field the total air pressure can be divided into the normal pressure P of the atmosphere, which is constant, and a varying term $p_{\sim}$ due to the sound vibrations, the so-called sound pressure.

The following requirement is made of a good microphone. The amplitude of the EMF excited by the sound pressure must be directly proportional to the amplitude of the sound pressure for every frequency $\omega/2\pi$ in the frequency range to be reproduced and the proportionality factor must be independent of the frequency. The amplitudes occurring are usually small enough to satisfy the first condition. In this article it will be explained how it is possible to make the proportionality factor indepent of the frequency.

In the first place we shall discuss the conversion of the motion of the membrane into an EMF, which involves the classification of microphones according to their electrical behaviour. We shall then deal with the different devices for the conversion of the air vibrations into motion of the membrane. This involves an acoustic classification of microphones. Finally the different useful combinations of electrical and acoustic characteristics and several models of different types of microphones will be described.

Electrical classification of microphones

EMF is dependent upon the deviation of the membrane.

In the classic *carbon microphones* (*fig. 1*) a deviation $x_\sim$ of a membrane M causes a change in the transition resistance between grains of

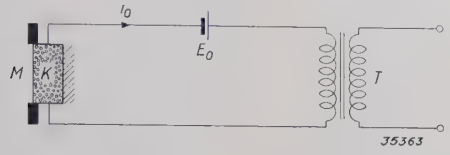

Fig. 1. Electrical circuit of a carbon microphone. M membrane, K grains of carbon, E_0 constant EMF, T transformer from which the alternating voltage of the microphone can be taken.

carbon which are enclosed in a container K. For sufficiently small deviations of the membrane the change in resistance ΔR is proportional to the deviation:

$$\Delta R = C x_\sim \quad . \quad . \quad . \quad . \quad . \quad . \quad . \quad (1)$$

where the proportionality factor C does not depend upon the frequency. The constant EMF E_0 applied to the microphone circuit gives a current $i_0 = E_0/R_0$ when the total resistance of the circuit is R_0. The small change in resistance ΔR of the microphone is therefore equivalent to an alternating EMF in the microphone circuit:

$$E_\sim = i_0 \, \Delta \, R = C \frac{E_0}{R_0} x_\sim \quad . \quad . \quad . \quad (2)$$

The relation between the EMF $E_\sim$ and the deviation $x_\sim$ of the membrane is thus independent of the frequency.

When a *piëzoelectric crystal plate* is stretched or compressed, electrical charges occur upon the side surfaces. If such a crystal C (*fig. 2*) is introduced between a rigid wall and a membrane which is set in motion by sound vibrations, an EMF $E_\sim$ is excited in the crystal which is proportional to the deviation $x_\sim$ of the membrane.

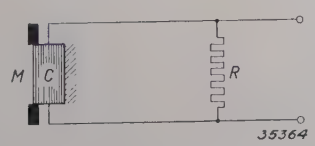

Fig. 2. Diagram of a piëzoelectric crystal, R resistance from which the microphone voltage generated can be taken.

This alternating EMF in turn can be made to excite an alternating current in an electric circuit.

In the case of the *condensator microphone* the moving membrane forms one of the plates of a condenser (*fig. 3*). The motion of the membrane causes changes in the capacity of the condenser.

When opposite charges have been put on the plates of the condenser over a resistance R by means of an electric battery, the changes in capacity lead to changes in voltage between the two plates, which in this case also have the same relation for all frequencies with respect to the deviations of the membrane.

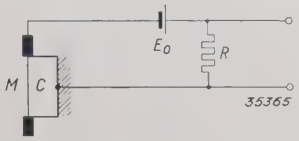

Fig. 3. Diagram of a condenser microphone. M membrane which forms a condenser C with the rigid wall. E_0 constant EMF, R resistance over which the alternating voltage of the microphone can be taken off.

For these three types of microphones the EMF generated is proportional to the deviation of the membrane, no matter how high the frequency. For satisfactory functioning of these microphones, therefore, it is only required that this deviation is proportional to the sound pressure for all frequencies. We shall discuss in the following the degree to which this requirement can be satisfied.

EMF depends upon the velocity of the membrane

In the case of an *electrodynamic microphone*, a membrane, ribbon or plate which is set in motion by the air vibrations is either itself electrically conducting or bears a conductor upon it. This conductor is placed in a constant magnetic field (*fig. 4*) and included in an electric circuit. Due to

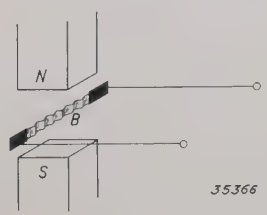

Fig. 4. Diagram of an electrodynamic microphone. N north pole, S south pole of a permanent magnet. B vibrating metal ribbon included in the circuit.

the motion of the conductor in the magnetic field the number of lines of force enclosed within the electric circuit changes:

$$N = N_0 + C x_\sim = N_0 + C x_0 \cos \omega t \quad . \quad (3)$$

where C is a constant and $\omega/2\pi$ the frequency. According to the law of induction, an EMF is hereby excited in this circuit, which is equal to the decrease per unit of time in the number of lines of force enclosed:

$$E_\sim = - \frac{\mathrm{d}N}{\mathrm{d}t} = - C \dot{x}_\sim = C \omega x_0 \sin \omega t, \quad . \quad . \quad (4)$$

where $x_\sim$ represents the derivative of the deviation with respect to time, *i.e.* the velocity of the membrane.

A small piece of soft iron which completes the magnetic circuit of a permanent magnet is fastened to the vibrating membrane of an *electromagnetic microphone* (*fig. 5*). Due to the motion of the

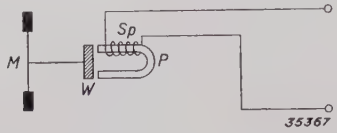

Fig. 5. Diagram of an electromagnetic microphone. *M* membrane to which a piece of soft iron is fastened which vibrates in the field of a permanent magnet *P* which is surrounded by a coil *Sp*.

membrane a varying magnetic field occurs which generates an EMF in a stationary electric coil surrounding the magnet and forming part of an electrical circuit. The situation in the case of such an electromagnetic microphone is quite similar to that in the case of an electrodynamic microphone, and in both cases an EMF occurs which is proportional to the velocity, the proportionality factor being is independent of the frequency. In order to obtain satisfactory reproduction for all frequencies with microphones which function on the electrodynamic or electromagnetic principle, the ratio between the velocity of the moving system and the sound pressure should therefore be independent of the frequency.

Acoustic classification of microphones

Pressure microphones

If one side only of the membrane *M* of the microphone is exposed to the variable sound pressure $p_\sim$ (*fig. 6*), one speaks of a pressure microphone.

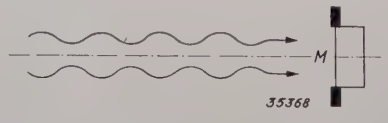

Fig. 6. Pressure microphone with moving membrane *M* placed in a plane sound wave.

In this case the force $K_\sim$ which the air vibrations exert upon the surface *S* of the membrane is equal to the product of this area and the sound pressure:

$$K_\sim = Sp_\sim = Sp_o \cos \omega t \quad . \quad . \quad . \quad (5)$$

When the mass of the membrane is *m*, the frictional resistance *r* and the stiffness *s*, the equation of motion of this membrane assumes the following form:

$$m x_\sim + r \dot{x}_\sim + s x_\sim = K_\sim = Sp_0 \cdot \cos \omega t \quad . \quad (6)$$

where $\ddot{x}_\sim$ represents the acceleration.

In such a moving system with one degree of freedom the greatest deviation for a given amplitude of the external force occurs when the frequency of the force is equal to the resonance frequency:

$$\frac{\omega_o}{2\pi} = \frac{1}{2\pi} \sqrt{\frac{s}{m}} \quad . \quad . \quad . \quad . \quad . \quad . \quad (7)$$

The way in which the amplitude of the vibrating system varies with the frequency differs very much according to whether the frequency in question is sufficiently far above or below the resonance frequency or in its vicinity. In these three different frequency regions each of the three terms in the left-hand member of equation (6) in turn plays the most important part, so that one may use the following approximations of equation (6) for the three regions:

$$\omega \gg \omega_o: m\ddot{x}_\sim = Sp_o \cos \omega t; \quad . \quad . \quad . \quad (8)$$

$$\omega \approx \omega_o: r\dot{x}_\sim = Sp_o \cos \omega t; \quad . \quad . \quad . \quad (9)$$

$$\omega \ll w_o: sx_\sim = Sp_o \cos \omega t; \quad . \quad . \quad . \quad (10)$$

In the neighbourhood of the resonance frequency, therefore, the sound pressure determines the velocity of the motion of the membran; for higher and lower frequencies the sound pressure determines the acceleration *viz.* the deviation.

In the case of carbon, piëzoelectric and condenser microphones, as we have already mentioned, the EMF depends upon the deviation of the membrane. As to the acoustic part of these microphones, care must therefore be taken that the ratio between the deviation and the sound pressure is independent of the frequency, *i.e.* equation (10) must be valid. These types of microphone must therefore be constructed as pressure microphones, and care must be taken that the resonance frequency for these systems with a single degree of freedom is made so high that the frequency region to be reproduced falls below it. If the resonance frequency should still lie in the region of the highest tones to be reproduced, a disturbing resonance will occur unless care is taken to make the damping sufficiently severe.

In the frequency region above the resonance frequency the ratio between the acceleration, ($\ddot{x}_\sim = \omega^2 x_\sim$) and the sound pressure is constant, according to equation (8). For the three types of microphone mentioned the amplitude of the EMF generated in the microphone circuit varies for high frequencies according to p_o/ω^2. The sensitivity thus decreases rapidly for high frequencies, as may clearly be seen from the resonance curve given in *fig. 7*.

A microphone working on the electrodynamic or electromagnetic principle will, according to equation (4), reproduce sound satisfactorily if the relation between the velocity of the membrane and the pressure does not depend upon the frequency. A pressure microphone may therefore only be used in these two types in the frequency region for which equation (9) is valid, *i.e.* in the vicinity of the resonance frequency. By making the mechanical damping large, provision may indeed be made that the frequency region in which the reproduction may be considered satisfactory becomes fairly wide, but the sensitivity then usually becomes too low, so that such a solution remains inadequate. If for certain reasons it is nevertheless desired to construct a pressure microphone according to the electrodynamic principle, it is advisable, in order to improve the reproduction of tones above and below this resonance frequency, to pass from the system with a single degree of freedom, which has only one resonance frequency to a system with several degrees of freedom which give rise to several successive resonance frequencies (*fig. 8*). Provision may indeed be made in this way that the sensitivity of the microphone remains practically constant over a wider frequency range, but the reproduction, especially of speech, is of poorer quality due to the maxima indicate the position of the resonance frequencies in the sensitivity curve of fig. 8. We shall therefore not consider such microphones further in this article, and consider only microphones with one degree of freedom.

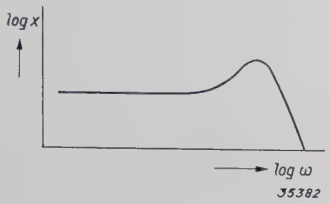

Fig. 7. Resonance curve of a membrane with one degree of freedom; the logarithm of the deviation x as a function of the logarithm of the frequency.

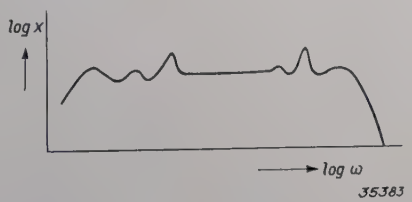

Fig. 8. Resonance curve of a system with more than one degree of freedom.

The sound pressure at a point does not depend upon the position of the surface element upon which one wishes to measure its effect. Therefore the action of a pressure microphone will not depend upon the position of the vibrating membrane with respect to the direction of propagation of the sound waves. A pressure microphone is therefore equally sensitive from all directions, so that the polar linear direction diagram of the sensitivity of this microphone is a circle. If the dimensions of the microphone are not small with respect to the wave length of the sound, the microphone itself distorts the sound so that deviations from this simple picture of the situation occur [1]).

Pressure-gradient microphones

If both sides of a membrane or a vibrating plate can be reached by the sound waves (*fig. 9*),

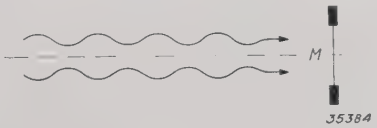

Fig. 9. Pressure-gradient microphone with a moving membrane M both sides of which are exposed to the air vibrations.

the latter will arrive at the front and rear sides with a certain phase difference. If the sound pressure on the front of the membrane amounts. for instance, to

$$p_1 = p_o \cos \omega t \quad . \quad . \quad . \quad . \quad . \quad . \quad . \quad (11)$$

and if the waves must cover a distance which is l cm longer in order to reach the other side, then for a wave length λ the sound pressure on the rear side of the membrane becomes

$$p_2 = p_o \cos (\omega t - 2 \pi l/\lambda) = p_o \cos (\omega t - kl) \quad . \quad (12)$$

where $k = 2\pi/\lambda = \omega/c$, c representing the velocity of sound. If the membrane has an area S, a force $K_\sim$ acts upon it which is the product of this surface and the difference in pressure $p_1 - p_2$:

$$K_\sim = S\,(p_1 - p_2) = Sp_o\,[\cos \omega t - \cos\,(\omega t - kl)] \quad (13)$$

Since this force is proportional to the pressure gradient, *i.e.* to the fall in pressure per unit of length, such microphones are called pressure-gradient microphones.

If the dimensions of the microphones are small compared to the wave length, *i.e.* if $l \ll \lambda$ or $kl \ll 2\pi$, the force becomes:

$$K_\sim \approx - Sp_o\, kl \sin \omega t \quad . \quad . \quad . \quad . \quad (14)$$

At a certain value p_o of the sound pressure the amplitude of the force acting on the membrane of a pressure-gradient microphone increases proportionally with k, *i.e.* proportionally with the fre-

[1]) *Cf.*: Philips techn. Rev. **4**, 144, 1939.

quency. The equation of motion for the membrane becomes:

$$m\ddot{x}_{\sim} + r\dot{x}_{\sim} + sx_{\sim} = K_{\sim} = -Cp_o\,\omega \sin \omega t \ldots (15)$$

which may be simplified in the following way for the frequency regions indicated:

$$\omega \gg \omega_o = \sqrt{\frac{s}{m}} : m\ddot{x}_{\sim} = -Cp_o\,\omega \sin \omega t; \quad . \; . \quad (16)$$

$$\omega \approx \omega_o \quad : r\dot{x}_{\sim} = -Cp_o\,\omega \sin \omega t; \quad . \; . \quad (17)$$

$$\omega \ll \omega_o \quad : sx_{\sim} = -Cp_o\,\omega \sin \omega t. \quad . \; . \quad (18)$$

By integration of (19) and (17) the following expressions are obtained:

$$mx_{\sim} = Cp_o \cos \omega t, \; . \; . \; . \; . \; . \quad (16')$$

$$rx_{\sim} = Cp_o \cos \omega t, \; . \; . \; . \; . \; . \quad (17')$$

which are valid for $\omega \gg \omega_o$ and for $\omega \approx \omega_o$ respectively. From formula (16 and 16′) it may be seen that for frequencies sufficiently far above the resonance frequency the ratio of the velocity of the membrane to the sound pressure becomes independent of the frequency. This is exactly what is required of a good electrodynamic (or electromagnetic) microphone, since in that case the ratio between the EMF excited and the velocity of the membrane is independent of the frequency. When a pressure-gradient microphone acting on the electrodynamic principle is used, very good reproduction can therefore be obtained for alle frequencies above the region of resonance.

If one desired to construct a pressure-gradient microphone on the principle of the carbon, piëzoelectric or condenser microphones, it could only be used for frequencies in the neighbourhood of the resonance, since the deviation only in that region is proportional to the sound pressure.

The gradient of the sound pressure depends upon the direction in which it is considered. Therefore in the case of a pressure-gradient microphone the induced EMF will depend upon the position of the membrane with respect to the direction of propagation of the sound waves. If in *fig. 10* we indicate the front and rear sides of the membrane by the points V and A, for which points the largest possible difference of path l for the sound exists, then the difference of path when the membrane is turned through an angle α with respect to the direction of propagation of the waves becomes equal to $l \cos \alpha$. In formulae (12) and (14) l must then be replaced by $l \cos \alpha$, so that the induced EMF will also be proportional to $\cos \alpha$. If this EMF is plotted in a polar diagram as a function of the angle α, a directional diagram is obtained which consists of two circles touching each other (*fig. 11*).

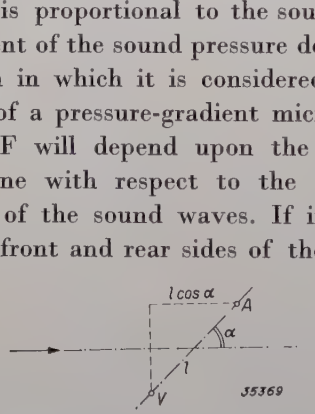

Fig. 10. A pressure-gradient microphone has the maximum sensitivity when the points V and A, which represent the front and rear sides of the membr ne, lie one behind the other in the direction of incidence of the sound, so that the difference in path is l for a plane sound wave. At an angle α this difference is only $l \cos \alpha$.

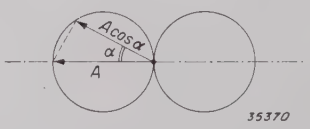

Fig. 11. The polar diagram of the sensitivity of a pressure-gradient microphone consists of two circles touching each other. At an angle α the sensitivity it is $A \cos \alpha$.

If the membrane is perpendicular to its position of greatest sensitivity, no EMF at all is induced, since the sound waves reach both sides of the membrane simultaneously and no difference in pressure occurs. Microphones with such a direction diagram may very well be used in rooms in which there is much noise and reverberation [2]) since this undesired sound in general arrives at the membrane with the same intensity from all directions while the sound to be amplified comes from a definite direction.

Combination of pressure and pressure-gradient microphone

If a pressure and a pressure-gradient microphone are connected electrically in series, a microphone is obtained whose EMF becomes equal to the sum of the EMF's of the two microphones. If for instance the EMF E_1 is generated in the pressure microphone and E_1 in the pressure-gradient microphone at its optimum position, then at any given position of the latter (at an angle α) the total EMF is:

$$E = E_1 (1 + \cos \alpha) \; . \; . \; . \; . \; . \quad (19)$$

The polar direction diagram then becomes a so-called cardioid (*fig.12*). For $\alpha = 0°$ the sensitivity, is greatest, while in the opposite direction ($\alpha = 180°$) the sensitivity would be zero since the pressure and pressure-gradient microphones give exactly equal and opposite EMF's with such orientation. Advantage may be taken of this characteristic when it is desired to reproduce the sound from a given direction while suppressing that from another direction.

---

[2]) *Cf.*: Philips techn. Rev. **3**, 221, 1938.

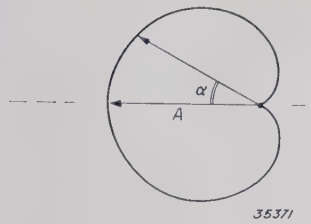

Fig. 12. The polar diagram of the sensitivity of a combination of a pressure and a pressure-gradient microphone having the same maximum sensitivity is a cardioid.

Technical models

After this general discussion we shall now deal briefly with four types of microphones constructed by Philips.

Carbon microphone

Carbon microphones may very well be used for the recording of the spoken word. While it is true that with very high sound pressures the magnitude of the contact surfaces between the grains is not proportional to the pressure exerted, so that the sound will be distorted, nevertheless carbon microphones have the advantage that they produce a much larger EMF than other kinds of microphones. A much smaller amplification is therefore needed with a carbon microphone, which makes it peculiarly suitable for simple applications.

The sensitivity of carbon microphones is higher, the larger the grains of carbon which is contains. The quality of the sound, however, diminishes at the same time, since the noise also increases with the size of the grains. Furthermore the carbon packs together somewhat in use, so that the sensitivity decreases with time. This can be prevented by tapping the microphone lightly.

Fig. 13. Carbon microphone, type 4225, special model for reporters. The microphone can be hung in the buttonhole of the coat.

An interesting use of the carbon microphone type 4225 is the reporter's microphone shown in *fig. 13*, which can be worn in the buttonhole. The relative sensitivity expressed as sound energy in db is shown in *fig. 14* as a function of the frequency,

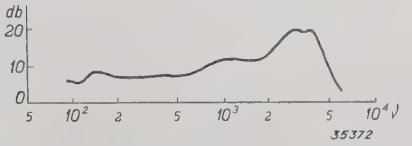

Fig. 14. Relative sensitivity of the carbon microphone, type 4225, expressed in db, as a function of the frequency.

from which it may be seen that the resonance frequency lies at about 3000 c/sec, while the sensitivity decreases rapidly with increasing frequency above 5000 c/sec. In *fig. 15* the dependence of the relative sensitivity in db on the direction is plotted in horizontal coordinates for frequencies of 1000 and 5000 c/sec, respectively. It may be seen (curve *a*) that the sensitivity at 1000 c/sec varies very little with the direction, so that the ideal pressure microphone is very closely approached. At higher frequencies, however, a much greater dependence on direction appears, as may clearly be seen in fig. 15*b*. This is a result of the fact that for frequencies of about 5000 c/sec the dimensions of the microphone are no longer small compared with the wave length.

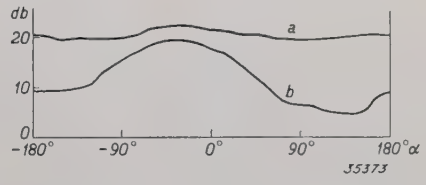

Fig. 15. Relative sensitivity of the carbon microphone, type 4225, as a function of the direction from which the sound is incident; *a*) at 1000 c/sec; *b*) at 5000 c/sec.

Crystal microphone

In the diagram of fig. 2 the air vibrations are transmitted by means of a membrane to a piëzoelectric crystal, Rochelle salt ($NaKC_4O_6$, $4H_2O$) for example. In crystal microphones constructed in this way care must be taken that the sensitivity for high frequencies does not vary irregularly with the frequency due to resonances in the driving mechanism. This has indeed been done in the crystal microphone type 9529, which is used for exemple in the table model of the so-called acorn microphone shown in *fig. 16*. The following point must, however, be kept in mind in connection with this

Fig. 16. Acorn model of a crystal, type 9 529, provided with a table standard. (height about 9 cm)

microphone. If a thin crystal plate of Rochelle salt is stretched in the direction of its length (*fig. 17a*) the two sides of the plate take on opposite charges, so that when it is used as a membrane (*fig. 17b*) and thus bent so that the two sides are stretched and compressed respectively they will then assume the same polarity. If two crystal plates are stuck together in such a way that their polarities are opposite (fig. 17*c*), a plate is obtained which assumes opposite charges on its two free sides upon bending [3]). Two such "bimorphous" crystal plates are mounted together in the manner shown in fig. 17*d*. Each of these plates experiences the effect of the sound pressure on the outer side only, so that the result is a pressure microphone.

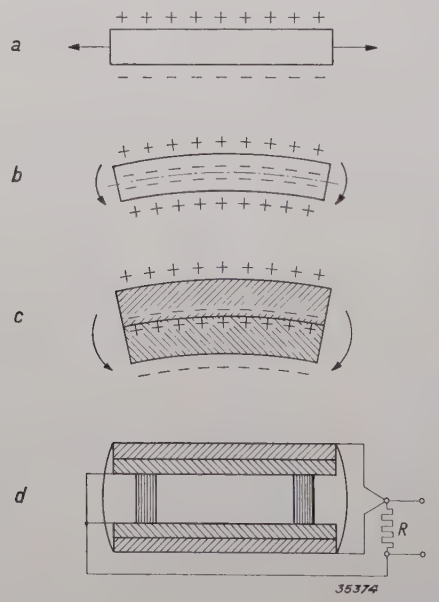

Fig. 17.*a*) If a piëzoelectric crystal plate is stretched opposite electric charges appear on its side surfaces. When compressed the charges are reversed.
b) Upon bending, the electric charges on the two sides have the same sign, which is opposite to that in the neutral layer whose length is not changed.
c) If two piëzoelectric crystal plates are fastened together with opposite orientation, the result is a so-called bimorphons crystal, which upon being bent assumes opposite charges on its two free surfaces.
d) The piëzoelectric crystal used in the crystal microphone, type 9 529, consist of two bimorphons crystals, one side only of which is exposed to the pressure of the air vibrations.

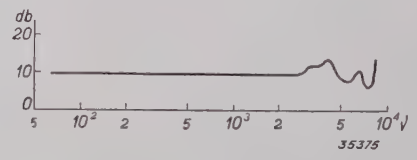

Fig. 18. Relative sensitivity of the crystal microphone, type 9 529, expressed in db, as a function of the frequency.

In *figs. 18* and *19* it is shown how the relative sensitivity in db depends, respectively, upon the frequency and the direction from which the sound strikes the microphone. For frequencies up to 5 000 c/sec the sensitivity is found to be practically independent of the direction, and above that frequency only slightly dependent on the direction.

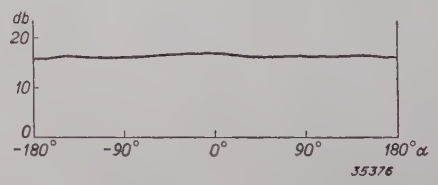

Fig. 19. Relative sensitivity of the crystal microphone as a function of the direction at 5 000 c/sec.

This is because of the small dimensions of the piëzoelectric crystal. The resonance frequency lies in the vicinity of 4 000 to 5 000 c/sec and presents no difficulties. In order to provide that not only the EMF $E_{\sim}$ generated, but also the terminals voltage $V_{\sim}$ shall depend only slightly upon the frequency, the external resistance R which completes the electrical circuit of the microphone must be made larger than the internal impedance of the microphone. Since the crystal behaves as a capacity C, the terminals voltage becomes therefore:

$$V_{\sim} = \frac{E_{\sim}}{\sqrt{1 + 1/\omega^2 C^2 R^2}} \cdot \cdot \cdot \cdot \quad (20)$$

This expression is only independent of the frequency when $\omega CR \gg 1$, *i.e.* for sufficiently high

[3]) According to patents of the Brush Crystal Company, Cleveland, Ohio.

frequencies, and increases linearly with the frequency when $\omega CR \ll 1$. If the microphone capacity is, for instance, $C = 2\,000$ $\mu\mu$F, and the external resistance $R = 1$ MΩ, at a frequency of about 80 c/sec the absolute value of ωCR will be approximately unity, so that $V = 0.72\ E$. Above 100 c/sec the terminals voltage does not change very much more with the frequency.

In the technical construction of these microphones care is taken that the microphone is well protected against the entry of moisture since the Rochelle salt crystals are not unaffected by water. Furthermore the microphone may not become too warm. If the Rochelle salt reaches a temperature above 55° C it loses its water of crystallization which is responsible for the piëzoelectric properties. When the temperature is lowered the water of crystallization does not recombine. The limit of 55° C is fortunately so high that it is never reached under normal conditions.

Ribbon microphone

In the table model of the ribbon microphone type 9 522 shown in *fig. 20*, a corrugated aluminium ribbon several microns thick is stretched between the pole pieces of a permanent magnet. The air vibrations exert their pressure on both sides of the ribbon which thus acts as a pressure-gradient microphone. Due to the motion of the ribbon in a magnetic field an EMF is excited in the circuit in which the ribbon is included, so that the microphone is of the electrodynamic type. According to the foregoing considerations, for a pressure-gradient microphone of the electrodynamic type the reproduction will be practically independent of the frequency when operating above the resonance frequency; formula (16′). In the case of this ribbon microphone the resonance frequency lies at about 50 c/sec, which is sufficiently low to ensure a practically constant sensitivity for the frequencies of speech and music.

Fig. 20. Ribbon microphone, type 9 522, opened (about 20 cm high and 9 cm broad).

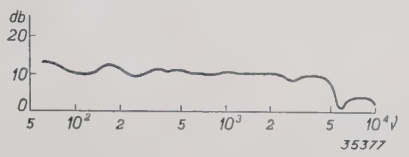

Fig. 21. Relative sensitivity of the ribbon microphone, type 9 522, expressed in db, as a function of the frequency.

It may be seen from *fig. 21* that the relative sensitivity of the ribbon microphone changes only slightly for the frequencies from 100 to 5 000 c/sec, while at 5 000 c/sec it begins to decrease. This may be explained as follows. The sensitivity of the microphone is given by the approximation formula (14). If, however, the product $kl = 2\pi\nu l/c$ becomes of the order of magnitude of 2π, (14) no longer holds and the succeeding terms of the series in the precise formule (13) must also be taken into account. From further considerations [4]) it is found that the sensitivity of the microphone will be practically independent of the frequency up to that frequency for which $kl = \pi$, *i.e.* where the product of k and the width $a = l/\pi$ of the pole piece is about unity. Now $k = 2\pi\nu/c = 2\pi\nu/34\,000$, so that with a width of the pole pieces of about one cm we may expect that the sensitivity will change little up to a frequency of 5 000 c/sec. For higher frequencies the sensitivity then decreases quite rapidly as may be seen in fig. 21. If it were desired that the sensitivity should decrease only at a higher frequency, this may be accomplished by making the pole pieces smaller, but under otherwise similar conditions this takes place, according to equation (14) at the cost of the magnitude of the sensitivity.

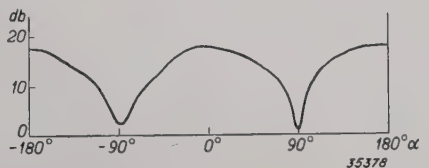

Fig. 22. Relative sensitivity of the ribbon microphone, type 9 522, as a function of the direction at 5 000 c/sec.

In *fig. 22* may be seen the manner in which the relative sensitivity of the ribbon microphone at 5 000 c/sec depends upon the direction from which the sound comes; for lower frequencies the dependence is practically the same. As must be expected

[4]) J. de Boer, Physica, **5**, 545, 1938.

in the case of a pressure-gradient microphone, the sensitivity to sound from directions perpendicular to that of greatest sensitivity is practically zero.

Coil microphone

In conclusion we shall describe a second type of pressure-gradient microphone of the electrodynamic type. In order to obtain a larger EMF the conductor which moves in a magnetic field consists of an electric coil in this case. *Fig. 23*

Fig. 23. Coil microphone, type 9 528, opened, rear view with back of magnetic circuit (cross section in fig. 24); diameter about 9 cm.

shows a coil microphone, the rear side of which has been opened. In the diagram of the cross section (*fig. 24*) it is shown how the coil (*Sp*) is wound upon a paper cap fastened to the membrane. The coil moves in a ring-shaped magnetic field; in the photograph the edge of the paper cap may be seen lying in the ring-shaped air gap.

Furthermore in fig. 23 it may be seen that the magnetic circuit is not closed over the entire circumference of the ring, but only over three parts by means of pieces of magnet steel *M*. The outer ring and the inner ring which form the north and south poles are made of soft iron. If the magnet steel had the form of a complete cylindrical shell, as is the case in the magnetic system of a loud speaker, the total number of lines of force cut by the vibrating coil, and thus also the EMF excited in the latter, would be larger. In spite of this that form is not chosen, in order to prevent the formation by the magnetic system of a resonating cylindrical space behind the membrane (open organ pipe), which leads to irregularities in the dependence of the sensitivity upon the frequency.

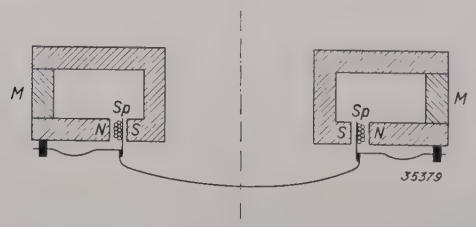

Fig. 24. Cross section of coil microphone. The coil *Sp* is wound on a paper cap the edge of which can be seen in fig. 25 in the air gap between the two poles. *N* north pole, *S* south pole. *M* are the three pieces of magnet steel, which provide the magnetomotive force for the soft iron ciruit.

By making the fastening of the membrane very flexible care is taken that the resonance frequency will lie below 100 c/sec. From this frequency, according to *fig. 25*, the relative sensitivity is found to depend little upon the frequency, up to about 5 000 c/sec. The magnitude of the sensitivity is such that with a sound pressure of 1 dyne/cm^2 and an output impedance of the microphone of 500 Ω a voltage of 0.9 mV is obtained.

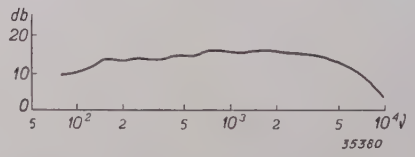

Fig. 25. Relative sensitivity of the coil microphone, type 9 528, expressed in db, as a function of the frequency.

The manner in which the relative sensitivity depends upon the direction from which the sound comes is shown in *fig. 26*. At a frequency of 500 c/sec, the sensitivity for directions perpendicular to that of greatest sensitivity is indeed approximately zero (fig. 26*a*) as is to be expected from a pressure-gradient microphone; for higher frequencies the minima are less pronounced (fig. 26*b*).

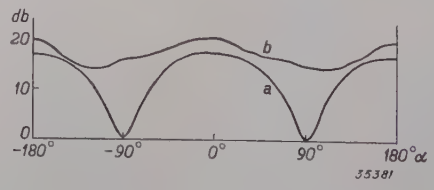

Fig. 26. Relative sensitivity of the coil microphone as a function of the direction. *a*) at 500 c/sec; *b*) at 5 000 c/sec.

THE ACCURACY OF MEASUREMENTS OF FIELD STRENGTH

by J. D. VEEGENS and J. J. ZAALBERG van ZELST. 621.317.42 : 621.396.81

A discussion is given of the main factors which affect the accuracy of measurements of the field of radio transmitters. A description is given of the way in which these factors are taken into consideration in the construction of the Philips recording field-strength meter. With this instrument it is found possible to measure the field strength with sufficient accuracy.

The strenght of the field of a radio transmitter is a quantity which is very important in transmitting and receiving technology, and which must therefore be known in many cases. In measurements for scientific purposes and also in certain cases such as the testing of transmitting and receiving installations which must precisely fulfill certain requirements as to efficiency, radiation or sensitivity, an accuracy of to within 1 per cent or less will be required. In most practical cases, however, it is unnecessary to measure the field strength with such great accuracy. Due to the influence of local or atmospheric conditions the field strength may vary so much that it will often serve no useful purpose to measure more accurately than to within 10 to 20 per cent.

The purpose of this article is to discuss the chief factors which affect the accuracy of measurements of field strength, and to indicate the method used in the construction and perfecting of the Philips recording field-strength meter [1]) of keeping the inaccuracies within satisfactory limits. It will be found that these inaccuracies are introduced during the calibration of the instrument, which process may be carried out at any desired moment by the user. For the calibration a concentrated EMF is introduced into the aerial circuit in place of the divided EMF which the field of a transmitter would induce therein. In the following it will be shown how care must be taken that the resistance through which this calibration EMF is introduced into the aerial circuit is practically free of induction, and that the voltage of the calibration oscillator is sufficiently sinusoidal. The influence will further be studied of the introduction of the calibration EMF into one of the windings of the loop aerial, while in conclusion the influence will be discussed of the capacities between the different supply connections and the windings. Before dealing with these points we shall first give a short discussion of the arrangement of the field-strength meter.

[1]) A detailed description of this apparatus (type GM 4 010) has already been given in this periodical: M. Ziegler, A recording field-strength meter of high sensitivity, Philips techn. Rev. **2**, 216, 1937.

The principle of the field-strength meter

The essential components of a field-strength meter are an aerial and a "voltmeter" for high-frequency AC voltages. The field whose strength is to be measured induces an EMF in the aerial, which is proportional to the field strength and also depends upon the form of the aerial. It is desirable that the relation between the field strength to be measured and the EMF excited thereby shall not depend upon the surroundings to any great extent. This can be realized with the help of a loop aerial, which moreover has the advantage of being less sensitive to interfering fields, since it receives only a small range of frequencies and its reception is directional. In order to cover a wide frequency range different loop aerials can be used. The EMF which is excited in the loop aerial causes between the terminals of the "voltmeter" a voltage difference which is a measure of the field strength.

The "voltmeter" consists of an amplifier with several tuned circuits by which the signal to be measured is amplified selectively, so that transmitters of a different frequency have no disturbing effect. The amplified signal is further rectified and conducted to an indicating instrument. The "voltmeter" also contains an attenuator with which it is possible to pass over to different measuring ranges for very divergent field strengths.

The calibration of the field-strength meter as a source of error

In technical manufacture it is practically impossible to make the properties of a loop aerial and the sensitivity of the voltmeter sufficiently constant. The properties of the aerial depend upon frequency, temperature and the degree of moisture of the air. The sensitivity of the voltmeter depends not only upon the frequency and the temperature of the surroundings, etc., but also upon the supply voltages of the amplifier. In order to eliminate this effect it is a practical necessity to be able to calibrate the instrument absolutely at any desired moment. In order to do this the whole field-strength meter might be placed in a radiation field of known

intensity, as is indeed done in special cases, in spite of the difficulties involved. In practice, however, it is impossible to apply such a "standard field" for every measurement which is carried out with the field-strength meter.

The customary method of calibration therefore is that of applying a known concentrated EMF to the aerial (substitution method), and *it is this method of calibration which forms the chief source of errors in field-strength meters*. If great accuracy is required in this method, it is not sufficient to know exactly the EMF generated, but one must also be certain that, within the desired limits of accuracy, this EMF will cause the same indication on the voltmeter as an equally great EMF induced by the external field. As will appear from the following this condition is not generally satisfied.

The application of a known calibration EMF

The calibration EMF is obtained by passing a current of known strength i_0 and variable frequency ν over a resistance ϱ which is connected in series with the aerial. In the substitution scheme of *fig. 1a* the total impedance of the aerial with the network connected with it is called Z. As to currents and voltages in the impedance Z this arrangement is absolutely equivalent to that of fig. 1*b*. In both cases a current $i_0\,\varrho/(\varrho + Z)$ flows through Z. The accuracy with which the calibration EMF E_0 is known thus depends exclusively upon that with which ϱ and i_0 are determined.

In order not to decrease the sensitivity of the field meter unnecessarily the calibration resistance ϱ, which is introduced into the loop circuit, must have a low value. In the Philips field-strength meter a value of about 0.1 ohm has been chosen. It is advisable for practical reasons that the same calibration EMF be obtained at the same value of i_0 for alle frequencies up to 30 megacycles per sec (*i.e.* a wave length of 10 m). This means that the influence of skin effect and selfinduction on the magnitude of the impedance of ϱ must be negligible. In the Philips field-strength meter a type of construction has been employed for this calibration resistance such that up to 50 megacycles per sec the impedance deviates less than 1 per cent from the DC value. This result is achieved by stretching 15 chrome nickel wires of a diameter 25 μ and a length 1 mm parallel to each other between two parallel copper discs (*fig. 2*).

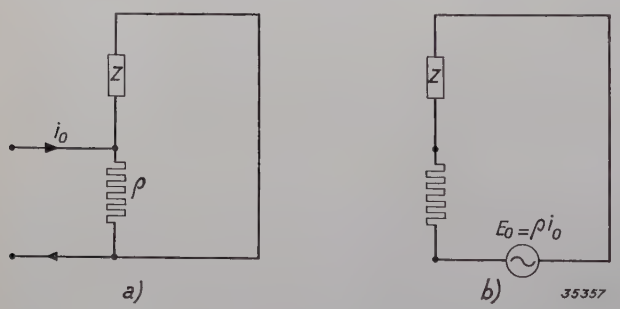

Fig. 1. Equivalent diagrams for the aerial with the network connected with it (total impedance Z) when fed with a calibration current i_0 for a calibration resistance ϱ, and with a calibration EMF E_0, in series with the calibration resistance, respectively.

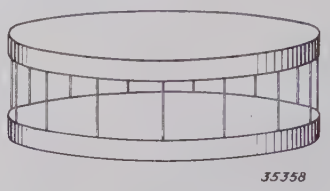

Fig. 2. Induction-free resistance consisting of two circular copper discs between the edges of which fifteen thin chrome-nickel wires are stretched.

The calibration current i_0 is provided by the calibration oscillator and contains a certain proportion of harmonics which might give rise to inaccuracies. The current is, however, measured by means of a thermocouple and a millivoltmeter, so that the influence of the different harmonics on the indication of the meter is manifested only in the form of correction terms which are related to each other as the squares of their amplitudes and not as the amplitudes themselves. The significance of this may be seen from the following example. If the amplitude of one of the harmonics is 10 per cent of that of the fundamental, and if we indicate the effective value of the fundamental component by i_0 and therefore that of the harmonics by 0.1 i_0, the indication of the millivoltmeter corresponds to a current of the magnitude:

$$\sqrt{i_0^2 + (0.1\,i_0)^2} \approx 1.005\,i_0$$

With a thermocouple the error is therefore only 0.5 %, while with a peak current meter in that case the error may amount to 10 per cent in both directions. The calibration oscillator may therefore easily be so constructed that the error in the magnitude of the calibration current may be neglected when it is measured thermally.

Influence of the asymmetry of the aerial circuit

By means of the field of a radio transmitter an EMF is excited in a loop which is small with respect to the wave length [2]). The EMF is proportional

[2]) Since in the case of the Philips field-strength meter the dimensions of the loop aerial are always small compared with the wave length of the field of radiation, it is unnecessary to consider the deviations which might occur if the substitution method were applied to aerials of larger dimensions.

to the intensity of the field and to the surface and number of windings of the loop. Since, however, a loop aerial as a whole also possesses capacity with respect to earth, without special precautions an EMF will also be induced in the aerial which depends upon the position of the loop with respect to the earth and to objects in its neighbourhood. The influence of this effect, the so-called aerial effect, can be avoided by arranging the aerial circuit so that it is absolutely symmetrical with respect to earth. To satisfy this condition a loop aerial can be used, which consists of two similar windings. As may be seen in *fig. 3*, however, the calibration resistance ϱ is introduced into one of the windings, thus causing an asymmetry in the aerial circuit. This resistance is, however, so small that the asymmetry which it causes in the aerial circuit is too slight to cause an appreciable aerial effect, but the calibration voltage is not introduced into the loop circuit symmetrically with respect to earth. If the voltage over the whole loop circuit were measured, it would be a matter of indifference where the EMF were introduced, but, as indicated clearly in fig. 3, the voltmeter V acts over only one of the two windings of the aerial. As a matter of fact this simplifies the construction and a calculation, which we are giving below, shows that is only involves a small error.

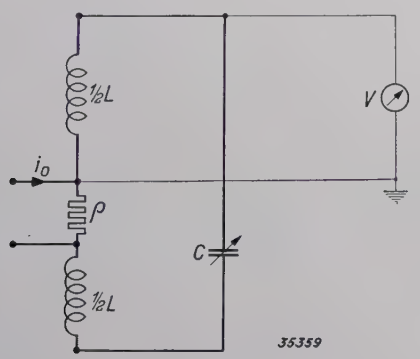

Fig. 3. The loop aerial consists of two symmetrical parts. The voltmeter V indicates the voltage on one of the two halves, which is a measure of the field strength around the aerial. The self-induction of the aerial is L, the tuning condenser C, calibration current i_0, calibration resistance ϱ.

Due to the resonance into which the loop circuit is brought, a calibration EMF E_0 applied *via* ϱ causes a much greater voltage Q_0E_0 over the winding of the loop to which the voltmeter V is connected. An EMF E induced by a transmitter in the loop circuit gives a voltage QE on the voltmeter. In general Q is not equal to Q_0. The relative error due to the asymmetrical introduction into the aerial circuit of the calibration voltage is now given by the relation $(Q - Q_0)/Q_0$. The larger the factors Q and Q_0, *i.e.* the higher the voltage over the coil with respect to that over the calibration resistance the less difference it will make whether or not the calibration voltage is included in the measurement by the voltmeter. On the basis of the simple diagram of fig. 3 in which further resistance in series or in parallel with the self-induction may be allowed, it may be calculated as a first approximation that $Q - Q_0 < 1/(8Q_0)$. The relative error thus becomes smaller than $1/(8\ Q_0^2)$. In the case of the loop aerials which are provided with the Philips field-strength meter for use in different frequency regions, the values of Q_0 lie between 20 and 150, so that in these cases the error may be neglected.

If high field strengths, greater than 50 mV/m, for instance, were to be measured, a high voltage might occur at the terminals of the "voltmeter". Such voltages, however, should be avoided because the amplifier valves would then operate outside their range of linearity, and there would no longer be a linear relation between the voltage supplied and the indication of the instrument. It would be better in such a case to introduce more resistance into the loop circuit. By giving the loop circuit a higher resistance, however, the factors Q_0 and Q are diminished, and it may indeed be necessary in that case to take into account the error due to asymmetry.

Influence of capacities between the different supply lines and windings

In fig. 3 only a very schematic representation is given of the actual aerial circuit. In *fig. 4* it may be seen that the loop aerial is placed at a distance of about 20 cm above the metal case in which are situated not only the voltmeter and the calibration oscillator but also the resistance ϱ and the condenser C. This distance is necessary in order that the metal case may not be able to disturb the field around the aerial. The presence of the lines which connect the aerial with the instrument, gives rise to considerable capacities between other parts of the aerial circuit as well as between the windings of the loop.

In order to discover the effect of these capacities upon the accuracy of the calibration method, further experiments were carried out with the field-strength meter. Each capacity in turn was artificially increased by known amounts, and in each the ratio Q/Q_0 was measured under the thus altered conditions. It is then found to be permissible in practical cases to assume that the capacities

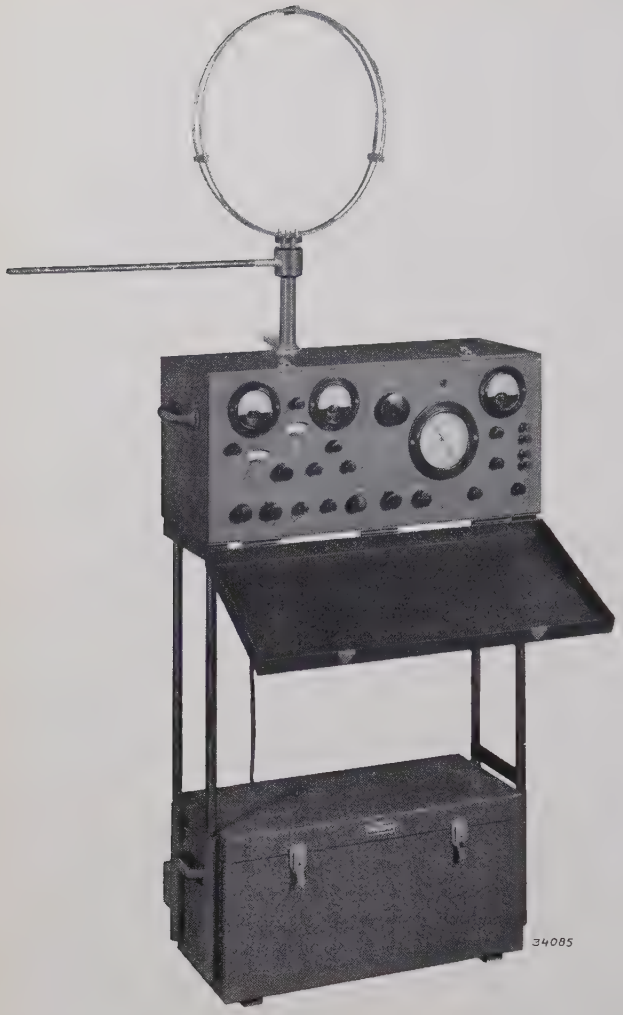

Fig. 4. The Philips recording field-strength meter type GM 4 010. Since the metal case in which the instrument is housed distorts the field in its immediate vicinity the loop aerial must be set up sufficiently far away from it.

between the connections, and for loops with two windings the capacity between the two windings also, are concentrated. In this way it becomes possible in the case of a loop aerial with two windings to carry out the calculations on the basis of the substitute diagram given in *fig. 5*. The capacity between the two windings of the loop aerial is represented by k. The six different capacities between the four supply lines, taken two at a time, are a_1, a_2, b_1, b_2, d and e. The capacity of the voltmeter V is hereby included in a_2. Here also, as in the case where the coupling capacities were neglected, it makes a difference in the voltage on the voltmeter V whether the EMF due to the field is induced divided over the whole aerial, or introduced in a concentrated form at a point of symmetry. If we again indicate the factors by which the voltage is increased by Q and Q_0, and if these are not too small, we find the following for the relative error:

$$\frac{Q-Q_0}{Q_0} \approx \frac{\omega^2 L}{4}(a_1 + a_2 - b_1 - b_2 - k), \quad . \quad (1)$$

where ω represents the angular frequency and L the total self-induction of the loop circuit. The errors found experimentally agree very well with this expression.

It may be concluded from the above that for a given loop the relative error will disappear if provision is made, by the addition of certain capacities, that

$$a_1 + a_2 - b_1 - b_2 - k = 0 \quad . \quad . \quad . \quad (2)$$

In order furthermore to avoid the aerial effect, these correction capacities are so chosen that they also bring about symmetry with respect to earth, thus: $a_1 = a_2$ and $b_1 = b_2$. According to the formulae the capacity d which is in parallel with the resistance ϱ has no appreciable effect on the accuracy. The capacity e is already compensated automatically in the tuning condenser C.

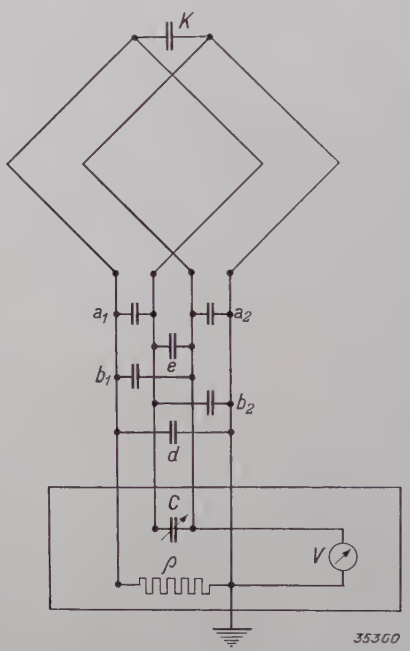

Fig. 5. Equivalent diagram for a loop aerial consisting of two windings. C tuning condenser, ϱ calibration resistance, a_1, a_2, b_1, b_2, d and e are the six capacities between the four supply lines taken two at a time. The capacity between the two windings is represented by k.

Loop aerial with more than two windings

With the Philips field-strength meter for use in the frequency region from 4 to 25 megacycles per sec (*i.e.* 75 to 12 m wave length), there are four different loop aerials, (*fig. 6*) each of which consists of two windings. The foregoing discussion may therefore be applied. If one desires to obtain a sufficiently large EMF at low frequencies without using loop aerials of very large dimensions, it is necessary to choose loops with a larger number of windings.

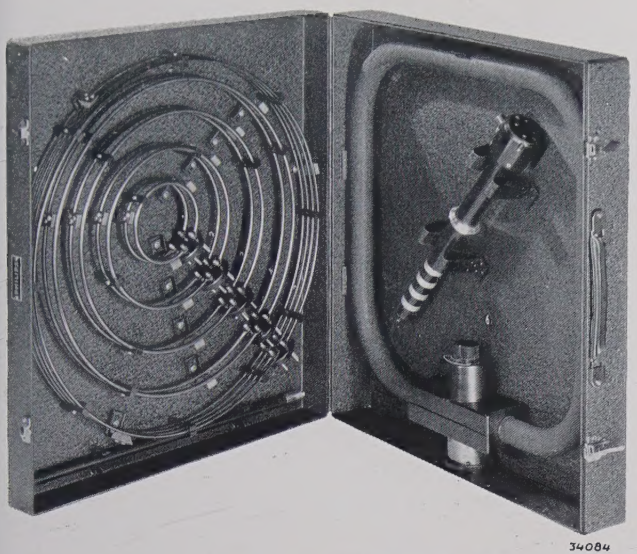

Fig. 6. The case containing the loop aerials provided with the Philips field-strength meter. In the left-hand section may be seen four double loops, which cover the frequency range from 4 to 25 megacycles per sec, as well as a loop consisting of four windings intended for 1,7 to 4 megacycles per sec. In the right-hand section is the loop aerial consisting of a large number of windings which may be connected in four different ways in series and in parallel with each other. This variable aerial serves the frequency range from 0,15 to 1,7 megacycles per sec.

The frequency region from 1.7 to 4 megacycles per sec is covered by a loop aerial with 4 windings, while finally for frequencies from 0.15 to 1.7 megacycles per sec (*i.e.* wave lengths from 2 km to 180 m) a loop aerial can be used which consists of a large number of windings connected in 4 different ways in series and in parallel with each other (fig. 5). Since according to the experiments the capacities for loops with more than two windings may not be considered concentrated, formula (1) cannot be applied to such cases. Since the situation is too complicated for simple calculation, it is better to determine the corrections experimentally, namely by comparison with a loop aerial with two windings whose errors are compensated in the manner here given. This has actually been done with the variable loop aerial which is a feature of the latest type of Philips field-strength meter. In the case of this aerial the corrections are indicated graphically as a function of the frequency.

Accuracy of measurement of the Philips field-strength meter

If we assume that the incidental errors in the results of the measurements which may arise in the setting, reading etc. are eliminated by repeating the measurement a sufficient number of times, there then still remain several other systematic errors besides those already mentioned which we shall here discuss.

The "effective height" of the loop aerial, that is the proportionally factor between the EMF generated and the field strength, is accurately known to within only 0.5 per cent. The inaccuracies in the circuit which provides for the rectification and amplification, and in the instrument which serves as indicator for the field-strength meter, together cause an error in the results of 2 per cent at the most. The attenuator which is used for passing over from one measuring range of the voltmeter to another may be the source of an inaccuracy of 0.5 per cent.

For the sake of comparison a summary of the magnitude of the errors already discussed is given in the following. The occurrence of the aerial effect may cause an error of 1 per cent. Due to the dependence of the calibration resistance ϱ on the frequency a maximum error of 1 per cent may be introduced. The occurrence of higher harmonics in the calibration current i_0 and the error in the instrument with which the latter is measured give an inaccuracy of 1 per cent in the results. Due to the incomplete compensation of the error caused by the mutual capacities (a_1, b_1, etc.) an inaccuracy of 1 per cent at the highest is caused.

If all the errors mentioned here should act in the same direction there would be a maximum error of 7 per cent. In general, however, these errors will not all act in the same direction, nor will they all assume maximum values at the same moment. Therefore one may in practical cases assume that an accuracy to within 4 per cent is obtained.

From the foregoing summary it is also clear that the fundamental errors adherent in measurements with this field-strength meter are of the same order of magnitude as the errors pertaining to the amplifier tubes and indicating instrument used. It is possible that the accuracy of the field-strength meter might be further enhanced by the use of precision meters. The practical utility of the method for measurements on the spot would, however, thereby be lost.

ABSTRACTS OF RECENT SCIENTIFIC PUBLICATIONS OF THE N.V. PHILIPS' GLOEILAMPENFABRIEKEN

1469: F. A. Kröger: Note on the wurtzitesphalerite transition of zincsulphide (Z. Kristallogr. A **102,** 136-137, Nov. 1939) (Original in English language).

Zincsulphide occurs in two enantiotropic modifications with a transition point at 1020 ± 5 °C. The velocity of transformation depends very much on the temperature and the dimensions of the crystals.

1470: A. Bouwers: The indirect radiograph (Radiology **33,** 357-362, Sept. 1939) (Original in English language).

The indirect radiograph obtained by means of a reduced picture of the screen image with a lens is compared with the direct image. With approximately equal contrasts the lack of sharpness of the indirect image is found to be approximately proportional to the cube root of the ratio between the intensity of the direct image and that of the reduced image. Since this ratio is inversely proportional to the square of the aperture, the relative aperture must be made as large as is possible without the reproduction faults becoming too large. If a tube with a rotating anode is used for the indirect image and one with a stationary anode for the direct image, the photographic quality of the indirect image is just as good as that of the direct image. In conclusion it is described how with a rotating anode exposures can best be made of the dimensions 24×32 mm, those of the ordinary miniature camera.

1471: E. J. W. Verwey and K. F. Niessen: The electrical double layer at the interface of two liquids. (Phil. Mag. **28,** 435-446, Oct. 1939) (Original in English language).

The variation of the potential is studied in the neighbourhood of an interface between two liquids, about which a small amount of electrolyte is distributed. The total potential difference due to the fact that one liquid has an excess of positive ions and the other an equal excess of negative ions is divided into two parts which are situated on either side of the interface. The largest part of the potential drop occurs in the liquid for which the product of ion concentration and dielectric constant is the larger. In general this product will have very different values for two substances, and if the total potential difference is not too great, it occurs almost entirely in the phase for which this product is the smaller. This does not, however, mean that the decrease in the density of charges on both sides of the interface need be very different. For larger total potential differences the partition of the potential drop between the two phases is somewhat less unequal, while for very large potential differences it approaches equality. For chemical applications of these considerations *cf.* **1467.**

1472*: M. J. O. Strutt: Modern short wave receiving technique (245 pages, Springer Berlin 1939) (German language).

Problems are discussed in this book which occur in the reception of radio waves of wave lengths from 50 to 0.2 m. The problems connected with receiving aerials and with the connection between aerial and receiving set are dealt with. Reliable methods of measuring currents, voltages and impedances at these short wave lengths are indicated. The problems are discussed which occur in the design of valves for amplification, mixing and rectifying voltages and currents at such high frequencies. In conclusion the important factors in the construction of complete receiving sets are discussed. The main text is kept as free as possible of mathematical analysis, which are, however, collected in an appendix for the sake of completeness.

1473: C. J. Bakker: Het splitsen van zware atoomkernen door neutronen. (The fision of nuclei of heavy atomes by neutrons). (Ned. T. Natuurk. **6,** 333-345, Dec. 1939).

In this address to the Netherlands Physical Society (Sept. 1939) a survey is given of the results obtained by the bombardment of nuclei of heavy atoms with neutrons. Hahn and Straßmann discovered in Jan. 1939 that uranium can be broken up in this way into radioactive isotopes of barium and lanthanum, and that no so-called transurania are obtained, as was formerly assumed. An investigation in the Philips laboratory has shown that the primary process of fision of uranium takes place in different ways. Furthermore analogous results were obtained with thorium. *Cf.* in this connection: **1410** and **1420.**

---

*) An adequate number of reprints for the purpose of distribution is not available of those publications marked with an asterisk. Reprints of other publications may be obtained on application to the Natuurkundig Laboratorium, N.V. Philips' Gloeilampenfabrieken, Eindhoven (Holland), Kastanjelaan.

1474*: H. Bremmer: Geometrisch optische benadering van de golfvergelijking (Geometrical optical approximation of the wave equation) (Handelingen 27e Ned. natuurk. en geneesk. Congres te Nijmegen, pp. 88-91, April 1939).

In this address before the Natuurk. en geneesk. Congres the well-known approximation formula of Wentzel, Kramers and Brillonin for the solution of a wave equation was derived in a new way. In the special case of one dimension an exact solution can be given in the form of a series, each term of which can be interpreted physically, and the first term of which is the well-known W.K.B. approximation.

1475*: F. A. Heyn: Het breken van uranium en thorium-kernen onder neutronen-bombardement (The breaking up of uranium and thorium nuclei upon neutron bombardment). (Handelingen 27e Ned. natuurk. en geneesk. Congres te Nijmegen, pp. 110-112, April 1939).

When uranium or thorium nuclei are bombarded with neutrons, among other products the radioactive rare gases krypton and xenon occur. The reactions of these rare gases are discussed in this paper (see also **1410**). Several reaction schemes are indicated.

1476*: J. F. Schouten: Het gebruik van de Fourieranalyse bij de interpretatie der onscherpe afbeelding. (The use of Fourier analysis in the interpretation of out-of-focus images). (Handelingen Ned. natuurk. en geneesk. Congres, pp. 110-119, April 1939).

It is shown in this paper that to a certain degree the exact form of an object can be deduced from an out-of-focus image by making use of a theorem of Fourier analysis. An example is the reconstruction of the exact shape of a spectral line from the poorly defined image which occurs due to the finite width of the slit. A semi-electrical arrangement is demonstrated with which the true line form can immediately be obtained from the apparent one and can be made visible on a cathode-ray oscillograph.

1477*: J. H. van der Tuuk: Metingen in verband met de diepte-scherpte aan röntgenstralen voor spanningen tot 1 millioen volt (Measurements in connection with the depth of focus on X-rays for voltages up to 1 million volts). (Handelingen Ned. natuurk. en geneesk. Congres, pp. 198-201, 1939).

For the contents of this address the reader is referred to Philips techn. Rev. **4**, 153, 1939.

1478: A. Bouwers: La production des rayonnements pénétrants. (Acta Univ. int. contra cancrum, Paris **4**, 245-253, 1939). (Original in French language.)

Penetrating rays which may be used for the purposes of therapy are:

a) photons (x and γ-rays)
b) neutrons
c) electrons (β-rays).

β and γ-rays have natural sources while x-rays and neutrons are obtained artificially. Neutrons can be obtained by allowing natural γ-rays to act upon beryllium, for instance, or by accelerating the atom nuclei of helium or heavy hydrogen sufficiently and allowing them to act upon a plate of suitable material. The acceleration may be direct or successive.

Hard x-rays are produced with the help of generators on the electrostatic or on the cascade principle. A generator with sealed x-ray tube for 1 million volts is described. An important problem is the protection against undesired radiation. For x and γ-rays the methods are well-known. For neutrons materials containing much hydrogen can best be used, such as water or paraffin, and combining these with a thin layer of a substance containing boron (boric acid for instance).

1479*: J. H. van der Tuuk: Recente metingen aan harde röntgenstralen (Recent measurements on hard x-rays). (Ned. T. Geneesk. **83**, 5815-5819, Dec. 1939).

In this address before the Netherlands society for electrology and röntgenology a discussion is given of the degree to which differences could occur in biological action between x-rays of various hardnesses and between x-rays and neutrons. The production of neutrons and of very hard x-rays is discussed. In conclusion a detailed study is made of the physical properties of very hard x-rays, see also **1477***.

1480: A. Bouwers and J. H. van der Tuuk: Further experiments with x-ray tubes for high voltages up to one million volts. (Brit. T. Radiol. **12**, 658-666, Dec. 1939). (Original in the English language.)

An improved sealed x-ray tube for voltages to one million volts is described. If a filter of 2.5 mm

of copper is used, the radiation of 800 kV DC voltage and a tube current of 1 mA amounts to about 14 röntgen/min at a distance of 1 m from the focus. The half-value thickness of the radiation may with this tube amount to 103 mm copper or 4.2 mm lead. The thickness of the lead screen by which the intensity of the radiation is reduced to below the tolerance dose, amounts at 1 million volts and 1 mA to 9 cm for the primary radiation, for the radiation scattered in the body irradiated to only a few mm. Furthermore, the nature of the radiation 10 and 20 cm under the surface of the skin is investigated with the help of a water phantom. In conclusion the intensity and the hardness of the radiation in the direction of the incident electrons is measured and found to be considerably greater than in a direction perpendicular to this.

1481*: M. J. O. Strutt and K. S. Knol: Measurements of currents and voltages down to a wavelength of 30 centimeters. (Proc. Inst. Rad. Eng. **27**, 783-789, Dec. 1939).

This is an English version of an article originally written in German which was reviewed under **1430.**

1482: J. M. Stevels: De berekening van de kookpunten van eenvoudige verbindingen (The calculation of the boiling points of simple compounds). (Natuurwet. T. **21**, 256-262, 1939).

In this article a summary is given of the method by which the boiling points of simple organic compounds can be calculated from three different contributions to the cohesion of the compound. For the contents refer to **1407, 1408** and **1462.**

1483: W. de Groot: De internationale temperatuurschaal voor temperaturen boven 1000 °C. (The international temperature scale for temperatures above 1000 °C). (Ned. T. Natuurk. **7**, 34-48, Jan. 1940).

A critical discussion is given of the principle upon which is based the international temperature scale above 1063 °C, as defined by optical pyrometry. The accuracy of the measurements is discussed and a lisest of fixed points on the temperature scale, such as have been determined recently in different laboratories, is given. A further study is made of the uncertainty in the constant c_2 of the radiation formula of Planck.

1484: F. A. Kröger: Luminescence and absorption of zincsulphide, cadmiumsulphide and their solid solutions (Physica, **7**, 1-12, Jan. 1940). (Original in the English language.)

In the case of ZnS, CdS and ZnS-CdS solid solutions a new emission is found at a temperature of —180 °C. The emission bands found consists of at least five parts, lying at equal intervals: the boundary of the emission bands at the short wave end coincides with the boundary of the fundamental absorption bands at the long wave end.

The emission bands were thus explained as combination frequencies due to the transition of one electron with a vibration. With the help of these emission bands an several new absorption measurements it has been established that in the series of ZnS-CdS solid solutions the edge of the fundamental absorption region is continuously displaced from ZnS to CdS.

ZnO exhibits an emission and an absorption in the ultraviolet which are quite similar to those of ZnS and CdS.